STRUCTURE OF TURBULENT WAKES OF HYPERSONIC SPHERES AS INFERRED WITH ION PROBES

D. Heckman, et al

Defence Research Establishment

Prepared for:

Advanced Research Projects Agency
Army Missile Command

August 1972

DREV R-669/72
PROJ. 75-51-10

NON CLASSIFIÉ
UNCLASSIFIED

STRUCTURE OF TURBULENT WAKES OF HYPERSONIC SPHERES AS INFERRED WITH ION PROBES

D. Heckman and L. Sévigny

DEFENCE RESEARCH BOARD
CONSEIL DE RECHERCHES POUR LA DÉFENSE

Québec, Canada
August/août 1972

59 R

DREV R-669/72
PROJ. 95-51-10

NON CLASSIFIE
UNCLASSIFIED

STRUCTURE OF TURBULENT WAKES OF HYPERSONIC SPHERES AS INFERRED WITH ION PROBES

by

D. Heckman and L. Sévigny

This research was sponsored jointly by

The Defence Research Establishment
Valcartier
P.O. Box 880, Courcelette
Quebec, Canada

The Advanced Research Projects
Agency
ARPA Order 133
Monitored by the US Army
Missile Command
Redstone Arsenal
Alabama 35089
Contract DA-H01-69-C-0921

CENTRE DE RECHERCHES POUR LA DEFENSE
DEFENCE RESEARCH ESTABLISHMENT
VALCARTIER
Tel: (418) 844-4271

Québec, Canada

August/août 1972

RESUME

On a utilisé des doubles peignes transverses de sondes ioniques pour étudier la structure du sillage ionisé produit par une sphère de 2.7 pouces de diamètre, lancée à 14,500 pi/sec dans une atmosphère d'azote à des pressions de 7.6 torr et de 20 torr. Pour chacune des positions radiales occupées par une paire de sondes, on a noté la valeur de la variable aléatoire correspondant à l'endroit derrière le projectile où l'ionisation se manifestait pour la première fois de façon perceptible, celui où le premier tourbillon ionisé faisait son apparition, et finalement celui à partir duquel la turbulence devenait continue. La première de ces quantités nous a permis d'établir une ligne de démarcation délimitant la région ionisée du sillage. Cette ligne est située entre la frontière de l'écoulement non visqueux définie par Wilson à partir de photographies strioscopiques et celle du sillage électronique déduite des profils radiaux de la densité du même nom déterminée par un interféromètre micro-onde. Par ailleurs les données relatives au premier tourbillon ionisé ont servi à évaluer l'étendue de l'ionisation en sein du noyau turbulent du sillage. Il ressort de nos résultats qu'environ les 4/5 de la portion visible par strioscopie de ce noyau est ionisée. On a également pu, de façon identique, définir une frontière en partant des données se rapportant au point d'origine de la turbulence continue. Or il s'est avéré que cette dernière s'écartait peu de celle délimitant le noyau turbulent proprement dit laquelle correspond à un facteur d'intermittence de 50%. D'un autre côté la différence entre les résultats à 7.6 torr et ceux à 20 torr va dans le même sens que celle observée pour d'autres mesures faites au Centre de Recherches pour la Défense Valcartier (CRDV).

ABSTRACT

Survey arrays of ion probes have been used to study the structure of the ionized turbulent wakes of 2.7 inch diameter spheres flown at 14,500 feet/second in atmospheres of nitrogen at pressures of 7.6 and 20 torr. For various radial distances measured from wake axis, matrices of data points have been obtained giving random values of the axial distance behind the projectile at which ionization begins, the first ionized eddy occurs, and continuous turbulence begins. A wake radius separating the significantly ionized wake from the unionized wake has been obtained, and found to lie intermediate between the inviscid wake radius defined by Wilson from schlieren measurements and an electron density radius corresponding to the 1/e points of the electron density distribution defined by microwave interferometric measurements. A radius defining the extent of the ionized portion of the turbulent core has been determined; this radius is of the order of 80% of the schlieren radius of the turbulence core.

The continuous turbulence data can also be used to define a wake radius; this radius has been identified as the mean position of the turbulent interface for ionized eddies, because it is in agreement with estimates of the turbulent interface obtained by fitting the radial distributions of intermittency estimates prepared from independent 0.5 millisecond long segments of the ion probe signals. The radius corresponding to the mean position of the turbulent interface is within the schlieren radius of the wake core. In addition to determining the mean position of the turbulent front, the standard deviation of the interface has been established. These last data have been found to be in broad agreement with data derived from measurements of the wake edge using schlieren techniques.

The differences in the results obtained at 7.6 torr and 20 torr have been considered and found consistent with other experimentally measured data obtained at Defence Research Establishment Valcartier (DREV); the occurrence of a transitionary type behavior in the frequency content of the probe signals from the 7.6 torr results has been noted but not explained.

TABLE OF CONTENTS

1.0 INTRODUCTION

The study of hypersonic wakes is a relatively new extension of fluid physics research, having only become routinely possible with the introduction of high velocity light gas gun launchers into ballistic range facilities just prior to the 1960's (Reference 1). Most of the early experimental work in the field was concerned with the study of the growth of the turbulent core in the wakes behind hypersonic spheres and other bodies using schlieren flow visualization techniques in combination with fast photography (References 2 - 6), although attempts were also made to infer growth information from microwave cavity measurements (Reference 7). As an aid to the theoretician, the wake growth data has proved disappointing because of its insensitivity as an indicator of the validity of various theoretical models of turbulent diffusion in the wake (Reference 8). This has led to the demand for more precise information such as spatially resolved data of the velocity and density distributions in hypersonic wakes. Recently a large experimental program in the ballistic range facilities at DREV has been completed in response to those needs (References 9 - 13). This program featured 'point' or spatially-resolved measurements in contrast to the 'integrated' character of the measurements attributed to optical and microwave techniques. As a consequence, in addition to optical or schlieren wake radii behavior, there now are available experimental data on the radii associated with velocity, mass density, and temperature distributions, at least in the case of hypersonic sphere wakes (References 14, 15).

Recent experiments at DREV using a transverse array of electrostatic probes sufficiently wide-spaced so as to cover a region of wake comparable to the wake diameter have also produced wake radii data, particularly in the case of the wake velocity distribution (Reference 16). The survey array has also been used to make point measurements of the behavior of the turbulent interface in the wake of a hypersonic sphere, both as a function of radial distance and as a function of axial distance behind the projectile, for several hundreds of body diameters. These new data are presented in this report. Similar information has previously been available only indirectly from the measurements on the edges of wakes as recorded on schlieren photographs, as first reported by Schapker (Reference 17) and subsequently by Levensteins and Krumins (Reference 6).

2.0 EXPERIMENTAL TECHNIQUE

As viewed by a schlieren system, the average width of the turbulent core of the wake of a 14,500 feet/second hypersonic sphere is about 4 sphere diameters at an axial distance of 125 diameters and almost twice this value around 1000 diameters behind the projectile (Reference 18). The physical variables which characterize the wake have been shown to vary significantly across the core and in some cases this variation can be well approximated by a gaussian curve (Reference 15). Any technique

which intends to survey the behavior of some variable across the wake must consequently make many simultaneous measurements over an extent of wake comparable to the average width.

Figure 1 shows a transverse survey array of electrostatic ion probes, typical of those used to observe the wakes of 2.7 inch diameter hypersonic spheres. The array consists of eight basic elements, each containing two ion probes. The eight elements are distributed uniformly along a line perpendicular to the direction of the axis of flight and separated horizontally by at least 1.25 inches. Depending on the exact arrangement, the distance between the outermost probes in the array can be up to 10 inches, or almost 4 sphere diameters. The presence of two probes in each of the eight elements is related to the velocity measuring capability of the array (Reference 16); for the present studies, one probe per element would have sufficed.

The individual ion probes are formed from miniature solid-jacketed coaxial cable by stripping the outer jacket and teflon insulator so as to expose a 2 millimeter long segment of the 0.28 millimeter diameter gold wire central conductor. The probes are biased at minus 4 volts (with respect to ground) so as to collect positive ions. The bias to each probe is supplied by an operational type current-to-voltage preamplifier, located in the preamplibier box at the base of the survey array. The compensating electron current is collected by the external jacket of the coaxial probe and by the adjacent supporting metal structure, which are grounded. The plasma of the wake will assume a potential slightly positive with respect to the metal structure immersed in it, thus the difference between the potential of the probes and the plasma will actually exceed 4 volts in magnitude.

The amplifiers for the 16 probes in the array are all located in the same preamplifier box, which is wedge-shaped to minimize the reflection of the projectile shock wave system (Reference 19). The frequency response of the preamplifier, as measured with an equivalent probe at the input, is flat from dc to several hundred kilohertz. Each preamplifier drives a ten to twelve foot length of coaxial cable needed to transmit the probe signals to the exterior of the range tank. The bias voltage is then removed by subtraction in a type 'O' unit, and the residual ion current signal is amplified for transmission to the recording room. Recording is carried out by means of Tektronix 551 and 555 double beam oscilloscopes and Wollensak 35 millimeter Fastax cameras. Timing marks are introduced in the signal traces by means of Z-modulation of the oscilloscope beam at intervals of one millisecond; together with pulses from various trigger stations located in the range which are recorded on the edge of the film, these assist in sychronization in time of the signals from various probes. The same trigger stations are used to feed time delay units and calibrated high-sweep speed oscilloscope recording. By these means it is possible to link various features on the film traces to the time at which the projectile passed over the probes. As a consequence, each timing mark on the signal trace can be related to the time either before or after the instant of passage of the projectile. Equivalently,

using the measured velocity of the projectile, each timing mark can be associated uniquely to a point in the wake at a specific axial distance (measured usually in projectile diameters) behind the projectile. The array itself is carefully positioned with respect to the range axis before the launching of the projectile, while the actual flight line of the projectile is determined by a series of X-ray flash photographs and a calibrated catenary wire reference system. The radial distance of each probe from the axis of the wake is thus completely determined. Any point on the signals recorded by the probes thus corresponds to a given radial distance R/D from the wake axis and a given axial distance X/D behind the projectile.

One additional point deserves to be mentioned. The interior of the range in the neighborhood of the measuring station is lined with smoothly profiled fiberglas wedges, oriented so that the plane of symmetry of the wedges passes through the axis of flight. This treatment has been found experimentally to significantly attenuate the effects of the projectile shock wave system (Reference 19).

The interpretation of the current drawn to an ion probe in a continuum flow, while almost always a problem in using electrostatic probes (Reference 20), is not considered to produce a difficulty here. The current is dominated by the existence of charge density, but whether the fluctuations in the probe current are solely due to fluctuations in this quantity or also due in part to fluctuations in velocity or in temperature (Reference 20) is probably irrelevant. We wish mainly to consider whether the flow appears to be laminar or whether it is turbulent. We are also interested in certain wake size or growth data, particularly that related to the existence of charge density in the wake core. The presence of turbulence is assumed to simultaneously cause fluctuations in all the physical variables in the wake, so that, experimentally speaking, it does not matter which fluctuations dominate the probe current signals being observed.

3.0 OBSERVATIONS AND MEASUREMENTS

3.1 Qualitative Observations

Figure 2 presents signals recorded by each probe in a symmetrical transverse survey ion probe array consisting of eight 2-probe elements. These signals are typical of those obtained on firings of 2.7 inch diameter spheres at 14,500 feet/second in nitrogen at 7.6 torr (Figure 2a) and in nitrogen at 20 torr (Figure 2b). Each pair of signals, characterized by the same value of radial distance R/D, corresponds to the signals from a 2-probe element of the array. (Consequently, the two signals of a pair are very similar, except that the features on the signal from the upstream probe (the uppermost signal of a pair) lead the corresponding features on the signal from the downstream probe (the lower signal of a pair)). In Figure 2, the overall order of the pairs of signals

corresponds exactly to the geometrical order of the 2-probe elements across the survey array. As previously mentioned, the signals of Figure 2 were obtained with symmetrical arrays, so that the projectile passed somewhere near the vicinity of the pairs of probes in the middle of the array. This is evidenced by the small values of R/D (0.85 and 0.90) of the probes in the center of the array, compared to the larger values of the outermost probes.

Unfortunately the number of available recording channels was limited on these experiments. Since the greatest variation in ion density with axial distance occurs near the wake axis, the central probes (at small R/D values) experience the largest variation in probe current. At least two channels of recording at different sensitivities were assigned to each probe of the 4 probe pairs in the center of the array and one channel to each probe of the outermost 4 probe pairs; an additional channel at a different sensitivity for each probe would have provided an optimum recording arrangement. The signals presented in Figure 2 were selected particularly to show the beginnings of the signals in the case of the central probes. The gains shown vary by a factor of 20 from the central probes to the outermost and the choice is the result of experience. One other remark should be made regarding this figure. Normally the cameras which record the signals on 35 millimeter film do not run at exactly the same speed, so that 1 millisecond may represent a shorter or a longer length of film on one signal than on another. The different signals shown here were enlarged by varying amounts so that 1 millisecond along each signal corresponded to the same physical length. The time marks are accordingly in correspondence across the various signal traces, providing for a more orderly presentation. The amplitude of the signals are slightly distorted as a result.

The general features of the near wake behind a sphere or another blunt body travelling at hypersonic velocity have been observed using schlieren techniques (Reference 5). At small values of X/D, the turbulent core of a hypersonic turbulent wake is imbedded in a surrounding cylindrical stream tube of hot inviscid fluid which was shock-heated to very high (ionizing) temperatures by passage through the near-normal portion of the bow shock wave of the projectile. This hot, inviscid flow is surrounded in turn by the cold inviscid flow which passed through the oblique part of the bow shock wave. The turbulent core of the wake grows with axial distance; eventually the viscous wake core becomes so large that it breaks through the 'walls' separating the hot inviscid flow from the cold inviscid flow. For the conditions of the present experimentation, this breakthrough takes place at about 200 to 300 diameters (Reference 5). Subsequent to breakthrough, the turbulent core grows by engulfing the relatively cold gas which surrounds it.

The ionization in the wake is created by the same processes which generate the high temperature flow in the center of the wake, and is thus confined mainly to the turbulent core and to the surrounding high temperature inviscid flow. Consequently, an ion probe situated near the

axis of the wake but outside the core (whose initial diameter is less than the sphere diameter) should initially collect a fairly steady current from the laminar hot inviscid fluid surrounding the core, and subsequently should collect an increasingly fluctuating current as the viscous core grows over it. A probe located at a larger distance from the wake axis should initially be in the relatively cold inviscid unionized flow and should not collect any current; until suddenly it begins to collect a fluctuating current as the turbulent ionized core engulfs the probe some time after breakthrough.

Examination of Figure 2 indicates that the experimentally observed behavior of the pattern of current collection by a survey array of ion probes is in accord with the above picture. Looking at the signals obtained by the probes with the smallest R/D values (0.85 and 0.90), and taking account of the channel gains, we see that the probe currents indicate first a laminar region of intense ionization over the first 30 diameters or so behind the body. The smooth signals from the laminar flow are occasionally interrupted by a burst of fluctuations associated with a turbulent blob from the core thrusting out into the laminar flow. After 30 diameters, the signals from the probes at small R/D values become continuously fluctuating, indicating the core has completely immersed them.

Looking next at the signals from probes situated at roughly 1.4 diameters from the wake axis, we see that the flow is preferentially laminar until at least 100 diameters or so behind the projectile. Around this axial distance, intermittent bursts of fluctuations become more and more frequent, indicating turbulent flow is beginning to engulf these probes. Finally the signal becomes predominantly fluctuating.

When the probes are located at about 1.8 diameters from the wake axis, there is no current detected from the laminar inviscid flow at the sensitivities employed. Bursts of fluctuations begin in the axial distance range situated between about 150 and 200 diameters, with evidence of considerable amounts of laminar fluid interspersed in the flow, giving the signals a sawtooth-like appearance. And the same sort of behavior occurs as one looks at probes located even further from the wake axis (Figure 2).

We can conclude from a first examination of the patterns of ion probe signals such as those in Figure 2 that, qualitatively, the behavior of the signals is at least roughly in accordance with the behavior of ion probe signals what would be predicted from the schlieren studies (Reference 5) of blunt body wakes. It is well to note that this type of probe data is probably unique in the case of hypersonic sphere wakes. The next step is obviously to make systematic observations on the various features present in the probe signals and to make quantitative comparisons of the results with the published schlieren data.

(Another interesting, and in fact striking, feature of the data in Figure 2 is the difference in frequency content between the signals obtained at 7.6 torr and those obtained at 20 torr. We will return to this effect later in the text).

3.2 Measurements of Occurence Data

The ensembles of probe signals, one at 7.6 torr and the other at 20 torr, were next submitted to systematic measurement. In the case of probe signals from survey arrays such as that illustrated in Figure 1, the separation between adjacent probes is almost 0.5 diameter. Since the average space scale is less than this value (Reference 20), all the signals from a survey array were considered as being independent. Additional signals from various special purpose arrays (Reference 21) were also admitted to increase the size of the sample, provided the independent data criterion was satisfied. Taken all together, data from 17 survey array rounds and 8 special array rounds at 7.6 torr have been considered; as well as data from 6 survey array rounds and 3 special array rounds at 20 torr.

Figure 3 illustrates the type of 'occurrences' that can be observed in typical ion probe signals obtained in hypersonic sphere wakes. For a signal from a probe located at a radial distance R/D, one can note the axial distance X/D at which 'ionization begins', at which the 'first eddy' occurs, at which the fluctuation (or the turbulence) becomes 'continuous', as well as the additional 'frequency' effects at 7.6 torr. For each type of 'occurrence' one thus builds up a matrix of data points for the random variable X/D at which certain events occur for various values of R/D. Some of these 'occurrences' are better defined than some other types, and some of the results are of more interest than others. A few remarks on each type of observations are necessary.

Consider the observation on when 'ionization begins', and what is meant by that observation. The definition of IB (Figure 3) must be qualified as follows. In these experiments linear recording was employed. At a maximum, only 2 channels of recording per probe at different gains were normally available. The lowest gains were chosen so that given a normal placement of the projectile with respect to the probes, the portions of the signal just behind the projectile would be recorded as shown in Figure 3 without off-screen effects. The higher gain channels permitted the capture of additional signal at larger axial distances behind the projectile. Now at the smaller radial distances, the point at which the ionization begins is well defined, independently of any choice of channel gain. At very large radial distances, there is equally no problem in defining where ionization begins, because it obviously occurs simultaneously with the arrival of the first ionized eddy. At intermediate R/D values there is some problem, because when there is a finite current to the probe as it traverses the more weakly ionized portions of the hot inviscid laminar wake, the level of detection is dependent on channel gain. Since the optimum choice of gain (in this experiment) was aimed at recording the

eddies at as large a gain as possible without off-screen loss on one channel, with a higher gain on a second channel, the threshold level at which ionization was detected correspond to a finite percentage of the initial maximum fluctuation amplitude observed at each radial distance. As a rough estimate, ionization levels below about 10% of the maximum fluctuation could escape detection. Experimentally speaking, however, it does not appear from the results that a choice of gain based on the magnitude of the fluctuating part of the probe current has caused a problem as regards the determination of an effective point for the beginning of ionization.

Consider now, the decision as to when the 'first eddy' occurs. Here again, in choosing the first eddy, there could be a dependence on the choice of gain. An insignificant feature in the probe current signal can look very much more important at a gain 20 times larger. The criterion employed was a simple one and consisted of relating the size of the fluctuation to that of subsequent fluctuations. To be recognized as the 'first eddy', the size of the fluctuation had to be such that there was no doubt in identifying the fluctuation on a recording in which nearby large fluctuations took up the available scale or were even slightly off-scale. This criterion probably translates into a requirement that the minimum size of the first eddy had to be of the order of 5 to 10% of the size of the large fluctuations.

After the 'occurrences' of the detection of the beginning of ionization and of the detection of the first (ionized) eddy, the next characteristic to be studied was the behavior of the fluctuations in the probe current. The behavior of the fluctuations is argued to represent the behavior of the fluctuations of turbulence in the wake flow. In particular, the points where the flow became predominantly turbulent were recorded. To accomplish this judgment, reference must be made to those portions or segments of the probe signals where the fluctuations were either absent or at a relatively undetectable level compared to the size of neighboring fluctuations. These segments were designated as representing laminar wake flow. In Figure 3, arrows are drawn to designate portions of the typical signals which are relatively smooth or unvarying. (The letter 'L' is used to identify 'laminar' stretches of signal). The 'continuous turbulence' was said to exist from the point where the portion of fluctuating signal in the total signal exceeded 50%. More precisely, the continuous turbulence was taken as the axial distance at which began the fluctuation or a group of fluctuations satisfying the 50% criterion.

An additional effect involving continuous turbulence is believed to be present in the 7.6 torr data. As previously remarked, there is obviously a difference in the frequency content of the signals at 20 torr and 7.6 torr; in fact, inordinately large 'scales' occasionally are indicated at 7.6 torr by cross-correlating signals from axial pairs of probes. The additional difference is the fact that in the case of signals obtained in the wake at 20 torr, all frequencies are evident in the fluctuations as soon as they are first detected; but in the case of signals

obtained at 7.6 torr, there is a noticeable lack of the higher frequency components in the initial fluctuations. These higher components appear in the region between 100 and 400 diameters behind the sphere. Accordingly, in the case of the 7.6 torr signals, not only was the axial distance at which the fluctuations became continuous noted, but also the axial distance at which the higher frequency components seemed to first appear. Admittedly, this particular chore of decision-making was not clearcut nor lacking in a degree of subjectivity. Figure 3a illustrates a signal showing 'continuous turbulence' as having an initial low frequency segment, followed by signal where high frequencies were also present. (As will be discussed later, this phenomenon of the absence and then subsequent appearance of high frequency fluctuations was initially thought to be somehow connected with transition (Reference 15)).

3.3 Estimating Intermittency Factor

The concept of intermittency is most easily understood in terms of the character of the signal obtained by a probe in a turbulent fluid. If a probe, such as a hot wire, was immersed in a turbulent fluid, and the electrical signal from the probe was found to contain bursts of random signal variation separated by varying-length periods of zero-fluctuation signal, then the flow would be said to be intermittent. Intermittency at a point in a turbulent fluid can be estimated by the ratio of the time duration of the fluctuating part of the signal to the total time. In a turbulent wake, as in a turbulent jet, intermittency would generally tend towards unity on the axis of the flow and would fall towards zero as one moves away from the axis of the flow. The behavior of the intermittency factor in the wake is important for an understanding of the structure of the turbulent wake flow (References 8, 22) but almost no data has been published (References 6, 17, 22).

The raw probe current data from the survey arrays have been used to estimate the intermittency factors across the wakes of 2.7 inch diameter hypersonic spheres in both 7.6 and 20 torr nitrogen atmospheres. The analysis was carried out in the following way. As previously mentioned, each signal is divided into one-millisecond segments by a time mark generator. Based for convenience on these time marks, the signal of each probe (that provides an independent observation) has been divided up into 0.5 millisecond segments. Also as previously described, based on certain reasonable criteria, each signal has been separated into laminar and turbulent portions, depending on the absence or existence of fluctuations in the signals. The decision as to which category a segment of signal belonged was effected by scientifically-trained personnel, and admittedly allows a degree of subjectivity in the estimation process. (Figure 3a illustrates well some of the difficult decisions which are required. An estimate of the sensitivity of the deduced results could have been made by deliberately biasing the decisions towards the laminar side and then repeating with a bias towards turbulence, but no effort was available for this task).

Once the decision is made as to which portion of a 0.5 millisecond signal segment represents turbulent flow and which represents laminar flow, the intermittency factor for the signal segment can be calculated. For each signal one can construct a histogram-like time or axial distance history representing the value of this factor estimated over consecutive sections of wake, each one being about 32 diameters further behind the projectile than the preceding section. Since each probe in an array is situated at a different radial distance from the wake axis, each histogram-like wake intermittency history corresponds to a particular radial distance. Now the absolute location of the time marks is different for each round. Consequently, all the histogram-like data were sampled at 25, 50, 75, 100, etc. diameters behind the projectile, and radial distributions of intermittency factor estimates obtained at corresponding axial distances. Figure 4 shows two typical radial distributions of intermittency factor estimates. Such radial distributions are susceptible to analysis to determine the mean position of the turbulent front and the statistics of the scattering of the actual location of the front about the mean position.

Assume that the instantaneous location of the turbulent front Y(t) is described by a gaussian density function in the radial coordinate with respect to the wake axis. The two adjustable parameters in this function are δ/D, the normalized average position of the turbulent interface and σ/D, the normalized standard deviation of the interface.

Mathematically, the intermittency factor Γ can be written as

$$\Gamma(y) = \text{prob}\left[y \leq Y(t) \leq \infty\right],$$

where y is a variable representing radial position with respect to the wake axis

and Y(t) is a random variable representing the instanteneous location of the turbulent front.

Assuming the previously described probability function for Y(t), the intermittency factor becomes (Reference 23)

$$\Gamma(y) = \frac{1}{2}\left[1 - \text{erf}\,\frac{(y - \delta/D)}{\sqrt{2}\;\sigma/D}\right],$$

where

$$\text{erf}\,x = \frac{2}{\sqrt{\pi}}\int_0^x \exp\,(-\xi^2)\,d\xi.$$

The above expression has been used to fit the intermittency data generated at axial distance intervals of 25 diameters behind the spherical projectiles considered in this paper, and as a result, estimates

of the mean turbulent front position δ/D and of the standard deviation σ/D were derived. In passing, it is noted that the mean position of the turbulent front so-defined corresponds to an intermittency factor of 50%.

4.0 RESULTS

4.1 Ionization Occurrence Frontiers

The matrix of data points for the axial distances at which ionization was first detected at various radial distances of the ion probes is presented in Figure 5. One can consider that at each radial distance R/D, the data define a border separating the ionized wake from the unionized wake. As previously admitted, the exact location of this border is somewhat dependent on the choice of recording gains. Usually data such as those of Figure 5 are plotted as a function of X/D, the axial distance behind the projectile. However, as far as occurrence frontiers are concerned, X/D is a random variable, while R/D amounts to a variable whose value is fixed before the experiment. Since one normally plots the dependent variable on the vertical axis and the independent variable on the other axis, one obtains a graph where the familiar 1/3 growth law has been transformed into a cubic growth law. This is not merely a question of taste. It is of real importance to know which quantity is the independent variable if one plans to fit data. A regression of Y on X does not necessary give the same answer as a regression of X and Y (Reference 26).

Also shown on Figure 5 are different types of wake radius measurements (the occurrence frontier plotting format is not the standard way of plotting these quantities but is necessary here to allow comparisons to be made). The solid curves at the right of the graphs are the edges of the hot inviscid wake described by Wilson from his schlieren observations (Reference 5). The solid circles on Figure 5a give the radius defined from the 1/e points on the mass density defect distribution measured by Dionne and Tardif (References 13, 15). Both the inviscid wake and the mass density radii appears to be beyond the ionization frontier, at least to almost 400 diameters behind the sphere which produced the wake. The electron density radius (open squares) was defined by determining the 1/e points on an assumed gaussian distribution of wake electron density, where the parameters of the distribution have been determined from simultaneous dual channel microwave interferometric measurements on the wake (Reference 24). Also shown are several data points (open hexagons) representing the 1/e points on an assumed gaussian distribution of wake ion density as found by applying ion probe theory to the current distribution measured with survey arrays of ion probes (Reference 25). Except for Wilson's inviscid wake radius, all the data points seem to merge around 400 body diameters. This phenomenon is quite obvious at 7.6 torr. Comparing the results as a function of pressure, it appears that the ionization frontier radius is about the same at both 7.6 and 20 torr.

Qualitatively the data seem to make sense. The electron and ion density radii are smaller than the 'frontier' defined between the ionized and unionized wake. In turn this frontier is smaller than the mass density radius until at least several hundreds of body diameters, and in turn, the mass density radius is smaller than the inviscid wake radius defined at the boundaries between the hot and cold temperature flows in the wake.

The inviscid wake radius given by Wilson seems to collapse towards the wake axis for axial distances less than 10 diameters, but the ionization frontier data does not show a similar trend. At axial distances of the order of 1 diameter behind the projectile, the exact axial distance at which ionixation is detected can be in error by one or two body diameters.

4.2 The Extent of the Ionized Turbulent Core

The matrix of data points defining the axial distances at which ionized fluctuations or eddies first appeared on the signal of an ion probe at a known radial position is given in Figure 6. These 'first eddy' data points provide a measure of the maximum distance from the wake axis at which one can detect turbulent eddies carrying charge densities which are significant compared to the mean ionization levels in the turbulent core. In fact, these data mark the outer edge of the ionized portion of the turbulent core, and by fitting the data we can hope to obtain a wake radius defining the average frontier of the ionized portion of the turbulent core. This frontier should be the analog of that measured for the mass density eddies in the wake by the schlieren technique. In both cases, the frontiers give an indication of the extent of the ionized fluctuations or the mass density fluctuations. In the first case there can be voids in the ionization, and in the second case, particles of laminar fluid can be imbedded in the wake. The analogy is not perfect because in the case of ionization the probe provides a point measurement, while the schlieren is an integrated measurement. Nevertheless, the analogy could be quite close.

A two parameter power law expression of the form

$$(X/D)_{F.E} = a\,(R/D)^{b}$$

has been fitted to the data. This gives for the values of the parameters

$$a = 31.3, \quad b = 2.5, \quad P_{\infty} = 7.6 \text{ torr}$$

and

$$a = 47.2, \quad b = 2.2, \quad P_{\infty} = 20 \text{ torr}.$$

The 90% limits of confidence values (Reference 26) for the powers are respectively $2.3 \leq b \leq 2.7$ at 7.6 torr and $2.0 \leq b \leq 2.4$ at 20 torr. It thus appears that the average frontier of the ionized portion of the

turbulent core broadens faster than a cubic growth law. These results can be compared with the measurements of Lahaye and Doyon (Reference 18) of the extent of the turbulent core for 15,000 feet/second spheres using the schlieren technique to detect the outline of mass density fluctuations over an order of magnitude of variation in ambient pressure. They found the schlieren radius to be independent of pressure and to be given closely by

$$(R/D)_{SCHL.} = 0.4\ (X/D)^{1/3},$$

or

$$(X/D)_{SCHL.} = 15.6\ (R/D)^{3}.$$

Although their work was carried out in air wakes, there seems little reason to believe the result would be significantly different in a wake of pure nitrogen.

We have previously argued that the 'first eddy' measurements provide an estimate of the extent or the frontier of the ionized portion of the wake core which is analogous to the frontier of mass density fluctuations in the core as seen by the schlieren technique. The results of Figure 6 show that the extent of the ionized portion of the core is significantly less than the extent of the core defined by mass density fluctuations.

It has already been established by the measurement of the velocity, temperature, ion density and mass density distributions at DREV (References 14, 15, 16, 25) that the turbulent core of a hypersonic sphere wake is not uniformly mixed. In addition it has been established by several techniques (References 15, 21) that the scale sizes of the fluctuations are small and on the average of the order of 0.1 - 0.2 diameter compared to wake widths of 6 to 8 diameters. Examination of the behavior of families of space-time correlation curves obtained in the hypersonic wake behind spheres by using up to 5 probes in an axial array configuration has also indicated time scales in the moving coordinate system of considerable duration and turbulence intensities of 20% to 30% (Reference 27). The mixing processes that are taking place in the wake core are thus not so violent as to result quickly in a spatial uniformalization of physical properties, given the strongly peaked and initially different distributions of ionization, temperature, etc., in the near wake.

Comparing the results at the different pressures, it seems that the ionized core radius at 20 torr is less than the width at 7.6 torr. This could be taken as further confirmation that the fluctuations at 7.6 torr are larger in size than those at 20 torr. Now if one examines the fits, one finds that the 20 torr data indicate a smaller radius at small axial distances but that the exponent describing the

growth of the ionized core with radial distance is somewhat smaller. The two-parameter curve fit for the 20 torr measurements intersects the curve for the 7.6 torr measurements at about 400 diameters behind the projectile. This is roughly the same axial distance at which the radii of the velocity distributions measured at 7.6 torr and 20 torr in nitrogen coincided (Reference 16).

4.3 Continuous Turbulence

As described earlier in section 3.2, the notion of continuous turbulence was introduced to describe the condition of the flow when the ion probe signal became predominantly fluctuating. Continuous turbulence was defined to exist from the point where the portion of the fluctuating signal in the total signal exceeded 50%. In terms of an intermittency factor, this is equivalent to defining the point in time from which this factor exceeded 0.5. From our previous discussion of this quantity, it would appear the ensemble of the so-called ,continuous turbulence, data points should provide a means of estimating the position of the turbulent interface, written as δ/D in normalized coordinates.

The matrix of data points for the occurrence of continuous turbulence is shown in Figure 7 in a form similar to the presentations in Figures 5 and 6. Once again the data have been fitted by a 2-parameter power curve of the form

$$(X/D)_{C.T.} = a\,(R/D)^{b},$$

where

$$a = 56.3, \quad b = 2.2, \quad P_{\infty} = 7.6 \text{ torr}$$

and

$$a = 78.3, \quad b = 1.9, \quad P_{\infty} = 20 \text{ torr}.$$

The 90% limits of confidence values for the exponents are respectively $2.0 < b < 2.4$ at 7.6 torr and $1.6 < b < 2.1$ at 20 torr. Once again one finds a behavior similar to that obtained with the first eddy data: the fit to the 20 torr data indicates an exponent smaller than that of the 7.6 torr data. In this case too, the two curves overlap at about 400 diameters. A look at Figure 7 reveals that the radius is smaller for the case of 20 torr, similar to previous findings in relation with the detection of the occurrence of the first eddy. In terms of the intermittency factor; the immediate results indicate that the turbulent interface is situated closer to the wake axis at 20 torr than at 7.6 torr.

4.4 Appearance of High Frequency Components in the Fluctuations at 7.6 torr

As previously described, there is obviously a difference in the frequency content of the signals at 20 torr and 7.6 torr. Additionally, in the case of the signals obtained at 7.6 torr, there is a noticeable

lack of higher frequency components in the initial fluctuations, with higher frequency components appearing rather randomly in the region between 100 and 400 diameters in axial distance behind the spheres. Figure 8 shows a matrix of data points for the first occurrence of higher frequency components in the signal at 7.6 torr. So as to avoid picking up data points which were solely due to wake edge effects, only data points were allowed where there was a run of signals deficient in high frequencies before the point where high frequency components made their appearance. The data in Figure 8 may give some appearance of following the wake edge, but this is probably due to the fact that the choice of gains employed for the center probes resulted in lower sensitivities in the center of the wake. In turn, this resulted in signal levels falling below the minimum level required to give reliable data at smaller axial distances than near the wake edge, and a consequent loss of data points.

Almost all of the data points lie in the band of axial distance extending from 100 to 400 diameters, and as reasoned above, the distribution of data points would probably have been uniform, but for the problem of low recording sensitivities near the wake center. This indicates a type of transition is taking place in the character of the turbulence at 7.6 torr in this range of axial distance. According to the measurements of Wilson (Reference 28), transition from laminar flow to turbulence for the 7.6 torr firings ($Re = 2 \times 10^3$) should begin in the wake neck about 7 diameters behind the projectile, and once initiated transition takes place within a few diameters. The present transition-type behavior is noted, but we have no explanation. One can perhaps repeat the observation, made with respect to wake velocity distributions measured at 7.6 torr and at 20 torr (Reference 16), that the velocity radius was initially larger for the 7.6 torr data but that the radii for the two conditions coincided after roughly 400 diameters.

4.5 Intermittency

As previously described (Section 3.3), the intermittency data estimated by averaging over 0.5 millisecond long segments of probe signal have been distributed into radial distributions corresponding to axial distances at integer multiples of 25 diameters behind the projectile. These radial distributions have been fitted by an intermittency function developed by assuming that the actual position of the turbulent interface could be described by a gaussian density function with a mean position given by δ/D and a standard deviation of σ/D.

Figure 4 shows examples of the intermittency function fits to the radial distributions of intermittency at $X/D = 100$. Most of the data points are confined to within the radial position band extending from 0.8 to about 2.0 diameters. At 100 diameters behind the projectile the parameters of the intermittency function are fairly well determined. Figure 9 illustrates the confidence contours at 75%, 90% and 95% for the parameters δ/D and σ/D from Figure 4a for $P_\infty = 7.6$ torr N_2 (Reference 16) (Normally the results are quoted at 90% confidence). At several hundred

diameters behind the projectile however, the intermittency function extends to considerably larger radial distances than those in Figure 4; however, the band of data points remains restricted to the region extending from about 0.8 to 2.4 diameters. As a consequence the parameters determined from fitting the intermittency function to the data become less and less precise. This effect is evident in Figures 10 and 11.

Figure 10 shows the turbulent front position or the mean (50%) intermittency radius δ/D obtained from the various radial distributions of intermittency data. (A complete set of the radial distributions of intermittency factor estimates is given in Appendix A for P_∞ = 7.6 torr and in Appendix B for P_∞ = 20 torr N_2). The point at X/D = 25 diameters should be ignored, because the interval of axial distance over which the individual intermittency estimates were derived corresponded to 32 diameters.

From 50 to about 200 - 300 diameters behind the body, the turbulent interface data follows reasonably well the 1/3 power law growth as can be seen by comparing with the schlieren radius given by $0.4\ (X/D)^{1/3}$. In addition the data over the first 200 body diameters appear to be in agreement with the so-called continuous turbulence data at P_∞ = 7.6 torr as it can be confirmed by comparing Figure 7 and Figure 10. This last fact indicates that the continuous turbulence does in fact correspond to a wake radius which is a good approximation to the position of the turbulent front or interface as suggested in section 4.3.

The standard deviation σ/D of the scatter of the actual position of the turbulent interface about the mean position is given in Figure 11. The values deduced remain sensibly constant until axial distances exceeding 200 diameters, where they apparently increase although this may be solely due to a lack of fit resulting from the experimentally restricted band of radial distance over which the intermittency estimates are available. One undeniable fact emerges concerning the influence of pressure however. The standard deviation of the position of the interface at 7.6 torr is about 1.5 times the standard deviation measured at 20 torr. This observation is consistent with previous observations noting the fluctuation size and the wake radii measured at 7.6 torr to be greater than the corresponding variables measured at 20 torr, at least over the region of the first 400 diameters behind the projectile.

5.0 DISCUSSION

The present report would appear to re-emphasize the utility of the ion probe for the study of hypersonic wakes, despite the well known objections concerning the interpretation of current signals from continuum probes in flowing plasmas. By studying the structure of the fluctuating signals obtained by a survey array of ion probes, it has been possible to deduce valuable information concerning the structure of the turbulence in the wake not previously determined by other techniques.

Of the various data obtained, that concerning the location of the turbulent interface or intermittency radius for the ionized eddies is probably of major interest. By themselves, the data concerning the radial position of the front as obtained from fitting the radial distributions of intermittency estimates are not well determined over a large range of axial distance. However, by comparison between Figures 7 and 10, it appears that the continuous turbulence also leads to a wake radius corresponding to the position of the interface, and at 7.6 torr these results extend to almost 1000 diameters. Over the range of the measurements, the front lies within the schlieren radius of the wake.

The normalized standard deviation describing the extent of the position of the turbulent interface about the mean is shown again in Figure 12 for the data at 7.6 torr. Also shown in Figure 12 are data obtained at approximately Mach 1' by Schapker (Reference 17) and by Levensteins and Krumins (Reference 6) from measurements of wake edge statistics on schlieren photographs. The Reynolds number range, where the Reynolds number is based on projectile size and free system conditions, is very similar among the different measurements. It is apparent that the trend of the DREV data is similar to that of the other measurements, although in the region around 300 diameters, where the DREV intermittency measurements are very uncertain, the present measurements seem to lie high by a factor of 2.

The ratio σ/δ of the standard deviation of the interface normalized to the mean radius of the interface is given in Figure 13. Also shown are the measurements of Demetriades, Townsend and Grant of the ratio σ/δ for self-similar turbulent wake flows (Reference 22). In order for a wake to be self-similar, the ratio σ/δ should have a constant value (Reference 29). The data indicate, in effect, the non-similarity of the flow in the turbulent wake behind a hypersonic sphere in the first few hundred diameters.

The transitionary type behavior in the 7.6 torr results where higher frequency components only make their appearance in the probe signals between 100 and 400 diameters seems to be a real effect (not due to ion probe behavior) which is echoed in the larger extent of the ionized core at 7.6 torr, the larger extent of the velocity radius (Reference 16), the size of the turbulent scales (Reference 20) and the greater roughness of the wake as indicated by the normalized standard deviation of the interface.

Some other aspects of the results are not wholly satisfactory. The determination of the frontier for the beginning of ionization leaves much to be desired because the threshold level of ionization that is detected is defined in terms relative to the size of the fluctuations, rather than in absolute terms. Other work in progress (Reference 25) may enable this criterion to be made more precise. Again, the methods for deciding that certain segments of signal represented laminar flow while other segments represented turbulent flow were somewhat arbitrary in

conception and admittedly subjective in application. At 20 torr, the decisions were usually obvious, but in the case of the 7.6 torr signals, they were often particularly difficult and arbitrary. However, while possible in theory, to have studied the sensitivity of the results to the actual criteria employed would have demanded the computerization of the whole process, which was beyond the effort available for this task. In fact, the effort actually employed was probably reasonable given the amount of the data and the attainable statistical accuracy.

6.0 CONCLUSION

Survey arrays of ion probes have been used to study the structure of the ionized turbulent wakes of 2.7 inch diameter spheres flown at 14,500 feet/second in atmospheres of nitrogen at pressures of 7.6 and 20 torr. For various radial distances measured from the wake axis, matrices of data points have been obtained giving random values of the axial distances behind the projectile at which ionization begins, the first ionized eddy occurs, and continuous turbulence begins. A wake radius separating the significantly ionized wake from the unionized wake has been obtained, and found to lie intermediate between the inviscid wake radius defined by Wilson from schlieren measurements and an electron density radius corresponding to the 1/e points of the electron density distribution defined by microwave interferometric measurements. A radius defining the extent of the ionized portion of the turbulent core has been determined; this radius is of the order of 80% of the schlieren radius of the turbulent core.

The continuous turbulence data can also be used to defined a wake radius; this radius has been identified as the mean position of the turbulent interface for ionized eddies, because it is in close agreement with estimates of the turbulent interface obtained by fitting the radial distributions of intermittency estimates prepared from independent 0.5 millisecond long segments of the ion probe signals. The radius corresponding to the mean position of the turbulent interface is within the schlieren radius of the wake core. In addition to determining the mean position of the turbulent front, the standard deviation of the interface has been established. These last data have been found to be in broad agreement with data derived from measurements of the wake edge using schlieren techniques.

The differences in the results obtained at 7.6 torr and 20 torr have been considered and found consistent with other experimentally measured data obtained at DREV; the occurrence of a transitionary type behavior in the frequency content of the probe signals from the 7.6 torr results has been noted but not explained.

ACKNOWLEDGEMENT

The authors wish to acknowledge the continued interest and support of continuum electrostatic probe diagnostic for wake studies shown by Dr. A. Lemay, former director of the Aerophysics Division at DREV. M. Jacques de Carufel, a summer research assistant in 1970, participated in the initial phases of the analysis when the value of this work had yet to be established. Other contributions were made by M. A. Emond, M. J. Gauthier, and Mlle Carolle Proulx. The figures were prepared by Mme Marie-Paule Kirkwood and by Mlle Nicole Bérubé.

REFERENCES

1. "Ballistic-Range Technology", AGARDograph No. 138, edited by T.N. Canning, A. Seiff, and C.S. James published by the Advisory Group Aerospace Research and Development, North Atlantic Treaty Organization, August 1970.

2. Slattery, R.E. and Clay, W.G., "Measurement of Turbulent Transition, Motion, Statistics and Gross Radial Growth Behind Hypervelocity Objects", Physics of Fluids, Vol. 5, No. 7, pp. 849-855, July, 1962.

3. Knystautus, R., "Growth of the Turbulent Inner Wake behind 3-In. Diam. Spheres", AIAA Journal, Vol. 2, No. 8, pp. 1485-86, August 1964.

4. Clay, W.G., Labitt, M. and Slattery, R.E., "Measured Transition from Laminar to Turbulent Flow and Subsequent Growth of Turbulent Wakes", AIAA Journal, Vol. 3, No. 5, pp. 837-841, May, 1965.

5. Wilson, L.N., "Far Wake Behavior of Hypersonic Spheres", AIAA Journal, Vol. 5, No. 7, pp. 1238-1244, July 1967.

6. Levensteins, Z.J. and Krumins, M.V., "Aerodynamic Characteristics of Hypersonic Wakes", AIAA Journal, Vol. 5, No. 9, pp. 1596-1602, September, 1967.

7. Labitt, M., "Measurement of the Diameter of the Electronic Wake of Pellets, MIT Lincoln Laboratory Technical Report 342, January, 1964.

8. Lykoudis, P., "A Review of Hypersonic Wake Studies", RAND/RM-4493 ARPA, 1965, also AIAA Journal, Vol. 4, No. 4, pp. 577-590, April, 1966.

9. Heckman, D., Tardif, L. and Lahaye, C., "Experimental Study of Turbulent Wakes in the CARDE Free-Flight Ranges", Proceedings of the Symposium on Turbulence of Fluids and Plasmas, Microwave Research Institute Symposium Series, Vol. XVIII, Polytechnic Press (published by Interscience), 1969.

10. Lahaye, C., Léger, E.G., Dufresne, M., Doyle, H. and Boucher, P., "The Sequential Spark Technique: A Tool for Wake Velocity Studies in Ballistic Ranges", ICIASF'71 Record, pp. 33-43, presented to the 4th ICIASF Congress, Von Karman Institute, Rhode-Saint-Genèse, 21-23 June 1971.

11. Ellington, D., Park, K.R. and Desjardins, P., "Hypersonic Wake Studies using Cooled-Film Anemometer Techniques", ICIASF'71 Record, pp. 45-69, presented to the 4th ICIASF Congress, Von Karman Institute, Rhode-Saint-Genèse, 21-23 June 1971.

12. Heckman, D., Emond, A., Fitchett, A. and Sévigny, L., "Mean and Fluctuating Charge Density Measurements in Turbulent Hypersonic Sphere Wakes", ICIASF'71 Record, pp. 68-79, presented to the 4th ICIASF Congress, Von Karman Institute, Rhode-Saint-Genèse, 21-23 June 1971.

13. Dionne, J.G.G. and Tardif, L., "An Application of the Electron Beam Fluorescence Probe in Hyperballistic Range Wake Studies", ICIASF'71 Record, pp. 80-86, presented to the 4th ICIASF Congress, Von Karman Institute, Rhode-Saint-Genèse, 21-23 June 1971.

14. Lahaye, C., Jean, L. and Doyle, H., "Velocity Distributions in the Wake of Spheres", AIAA Journal, Vol. 8, No. 8, pp. 1521-1523, August, 1970.

15. Dionne, J.G.G., Heckman, D., Lahaye, C., Sévigny, L. and Tardif, L., "Fluid Dynamic Properties of Turbulent Wakes of Hypersonic Spheres", Proceedings of the AGARD Specialists Meeting on Turbulent Shear Flows, London, England, September 13-14, 1971.

16. Sévigny, L., Heckman, D. et Emond, A., "Détermination du Champ de Vitesse du Sillage d'une Sphère Hypersonique à l'aide de Peignes de Sondes Ioniques", Canadian Journal of Physics (à paraître).

17. Schapker, R.L., "Turbulence Front Statistics of Wakes from Bodies in High-Speed Flight", BSD-TR-65-158, Research Report 217, AVCO Corporation, June 1965, also "Statistics of High-Speed Turbulent Wake Boundaries, AIAA Journal, Vol. 4, No. 11, pp. 1969-1987, November, 1966.

18. Lahaye, C. and Doyon, P., "Growth Characteristics of Turbulent Wakes" (to be published).

19. Heckman, D., Lahaye, C., Podesto, B., Moir, L. and Robertson, W., "A Shock Wave Treatment for Ballistic Ranges", AIAA Journal, Vol. 9, No. 7, pp. 1355-1357, July, 1970.

20. Hedkman, D., Emond, A. and Sévigny, L., "Some Results of Electrostatic Probe Studies of Turbulent Hypersonic Wake Plasmas", AIAA Preprint No. 68-689, presented to the AIAA Fluid and Plasma Dynamics Conference, Los Angeles, June 24-26, 1968.

21. Sévigny, L. and Heckman, D., (to be published).

22. Demetriades, A., "Turbulent Front Structure of an Axisymmetric Compressible Wake", J. Fluid Mech. (1968), Vol. 34, part 3, pp. 465-480.

23. Blackwelder, R. and Kovasznay, L.S.G., "Large Scale Motion of a Turbulent Boundary Layer with a Zero and a Favorable Pressure Gradient", Interim Technical Report No. 2, Department of Mechanics, The Johns Hopkins University, Baltimore, Maryland, July, 1960.

24. Heckman, D., Sévigny, L., Doyon, P., Emond, A. and Fitchett, A., "Electron Density Behavior in the Wake of 14,500 feet/second Spheres", DREV R 680 (Unclassified) (to be published).

25. Sévigny, L., Heckman, D. and Caron, P., "Ion Density Measurements in the Wake of a Hypersonic Spheres", DREV R 670 (Unclassified) (to be published).

26. Draper, N.R., Smith, H., "Applied Regression Analysis", Wiley (1966).

27. Sévigny, L., "Exploration of Space-Time Correlation Functions", DREV TN 1844/69, October, 1969. (Unclassified).

28. Wilson, L.N., "Body-Shape Effects on Axisymmetric Wakes: Transitions", AIAA Journal, Vol. 4, No. 10, pp. 1741-47, October, 1966.

29. Corrsin, S., Uberoi, M.S., "Free-Stream Boundaries of Turbulent Flows", NACA Rept. 1244 (1955).

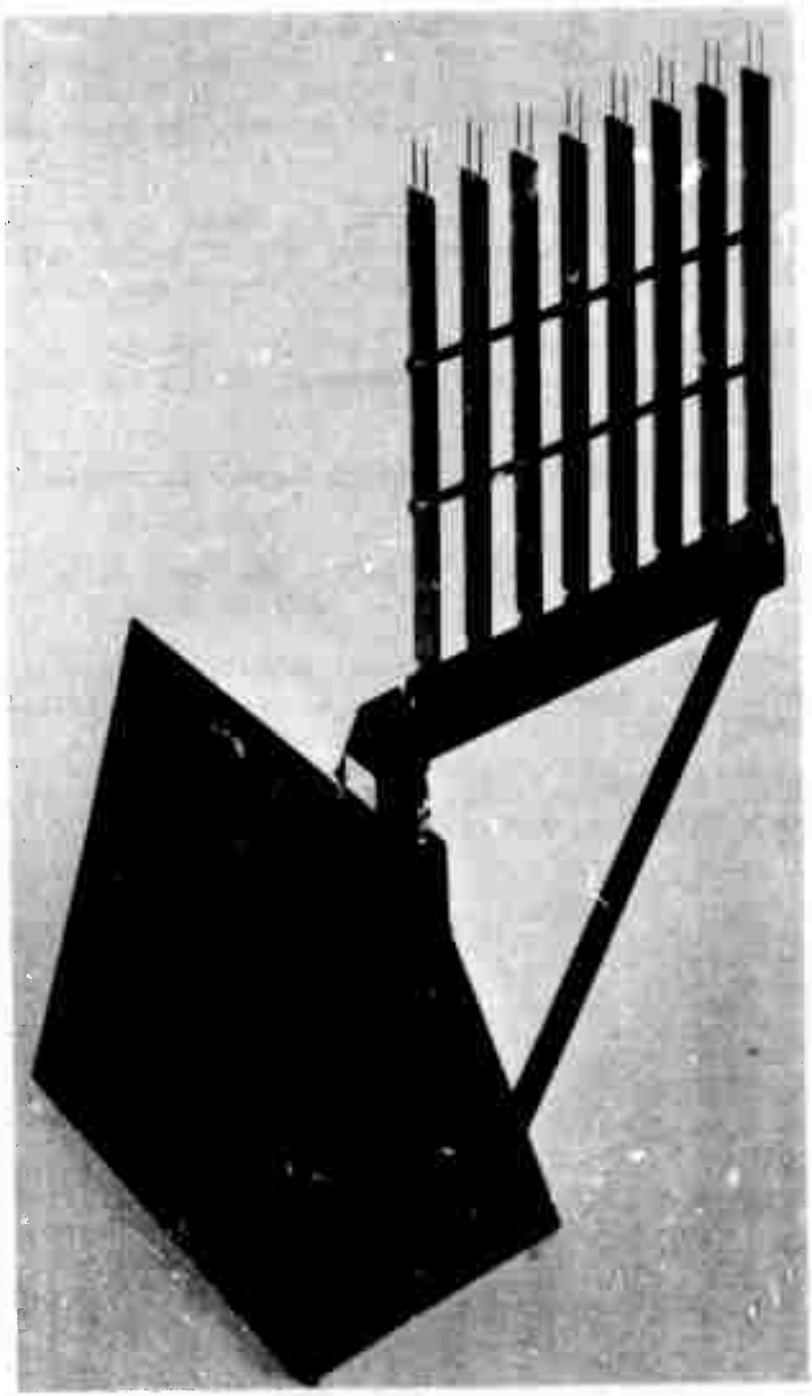

FIGURE 1

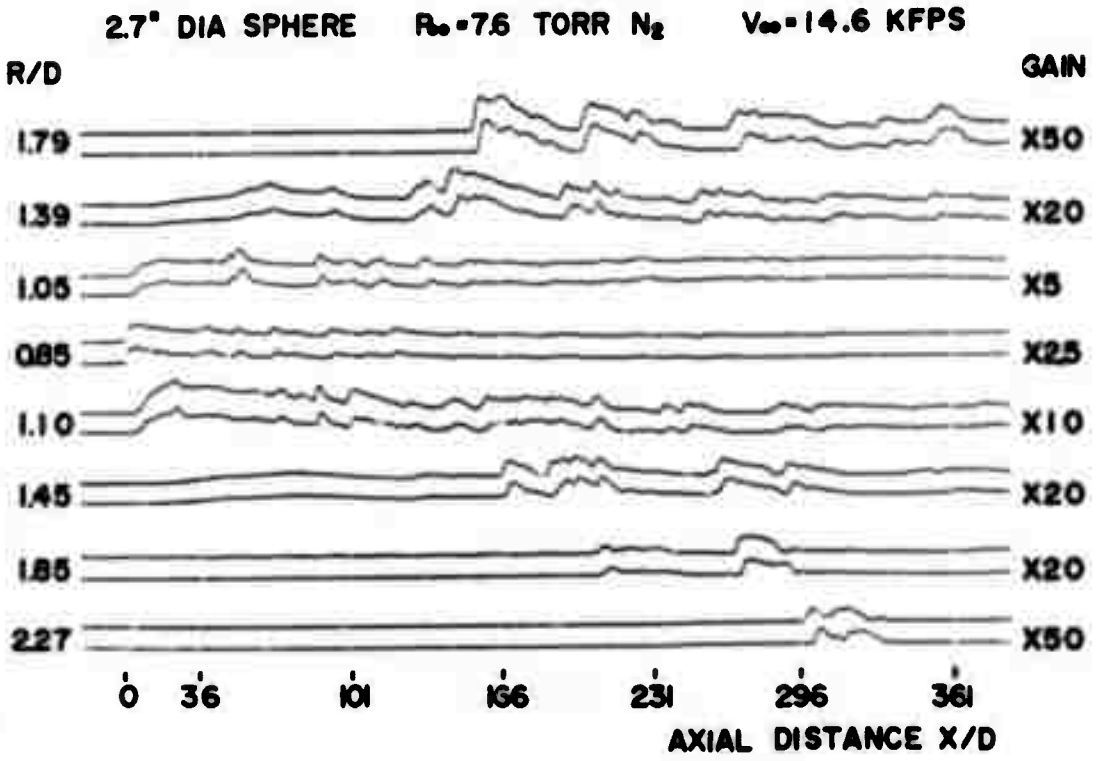

FIGURE 2a

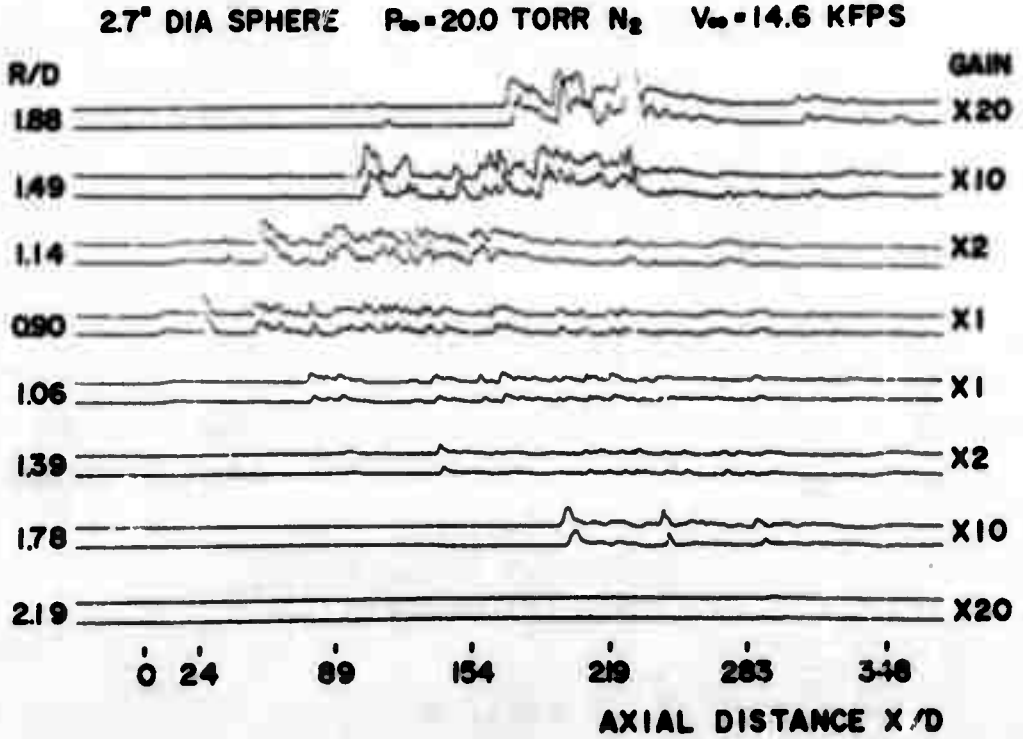

FIGURE 2b

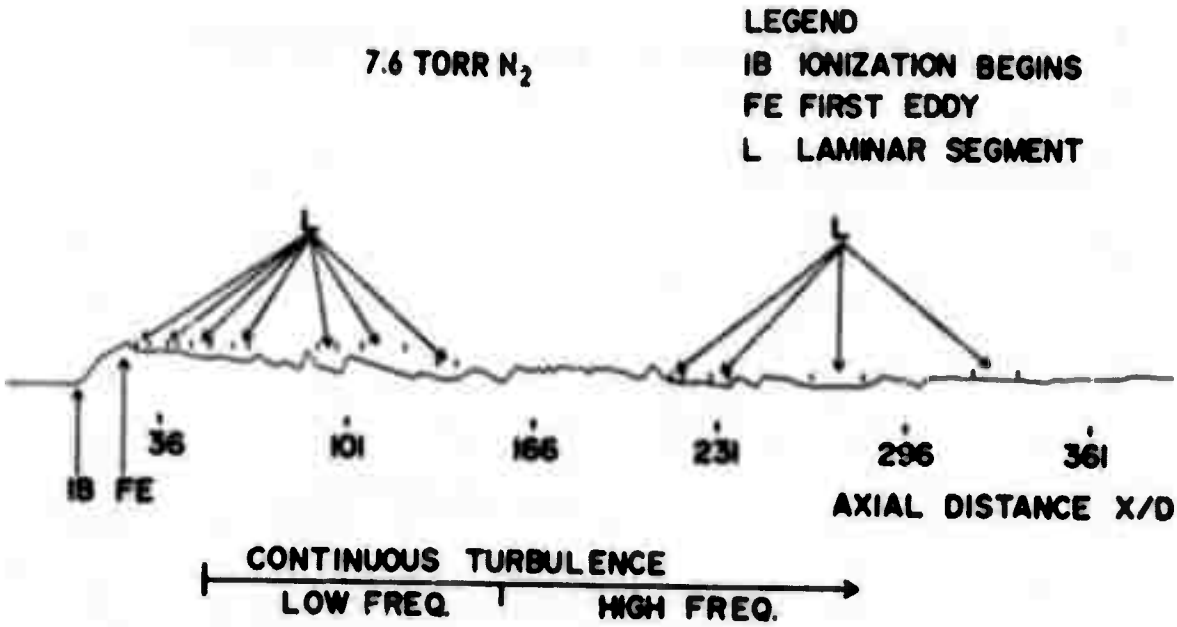

FIGURE 3a

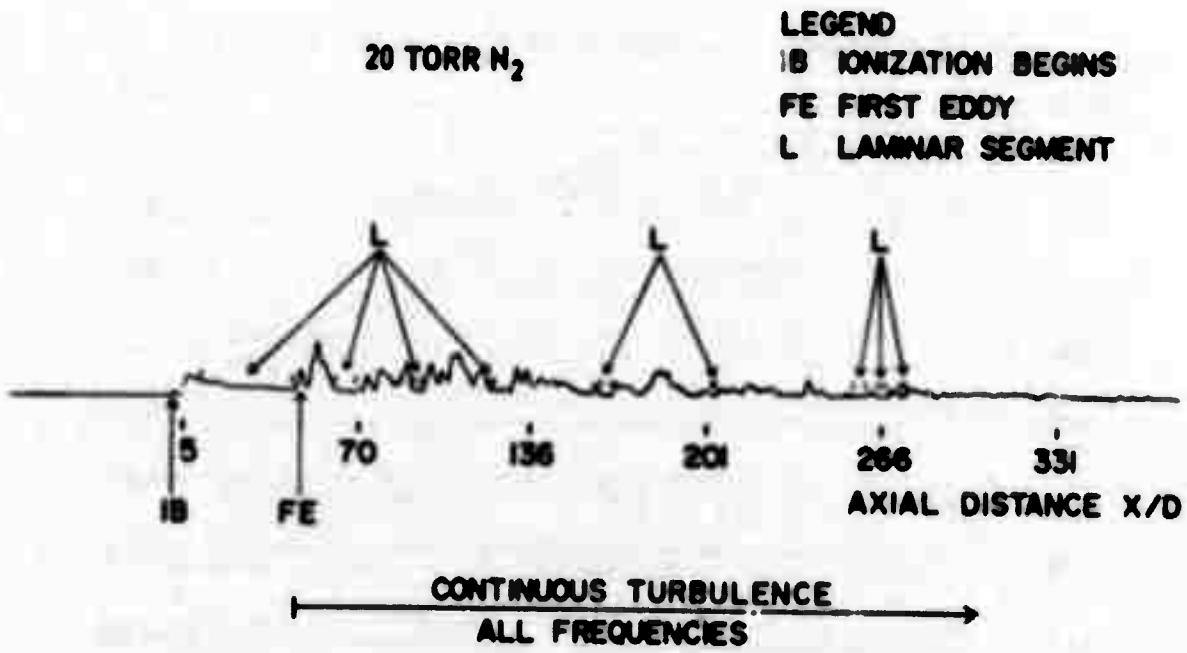

FIGURE 3b

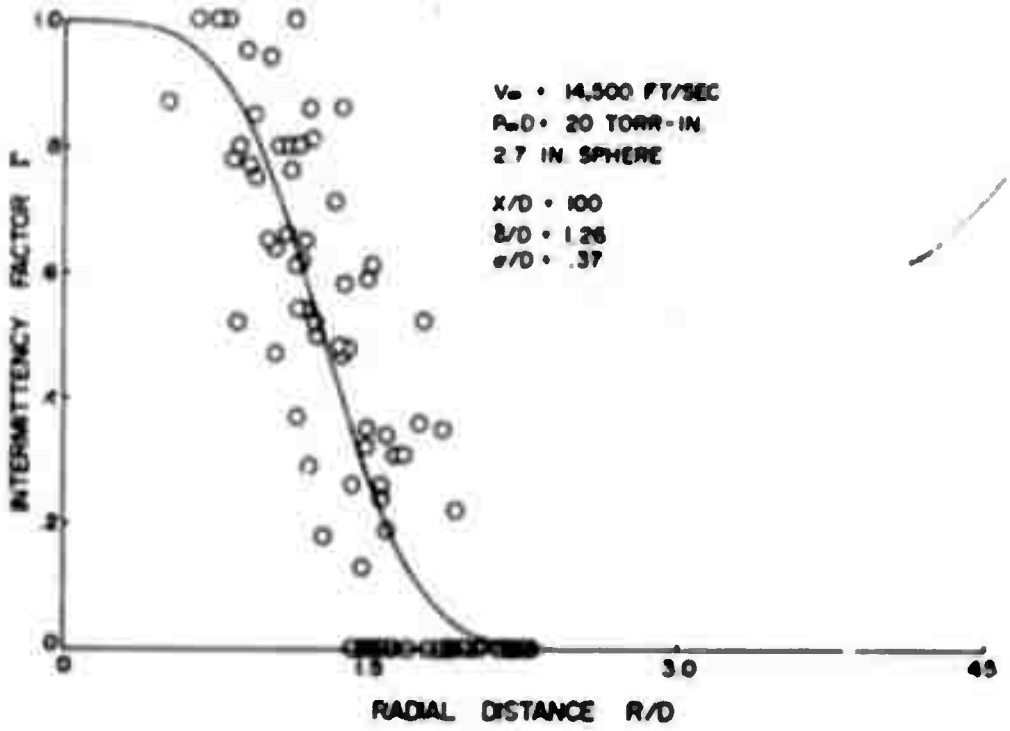

FIGURE 4a

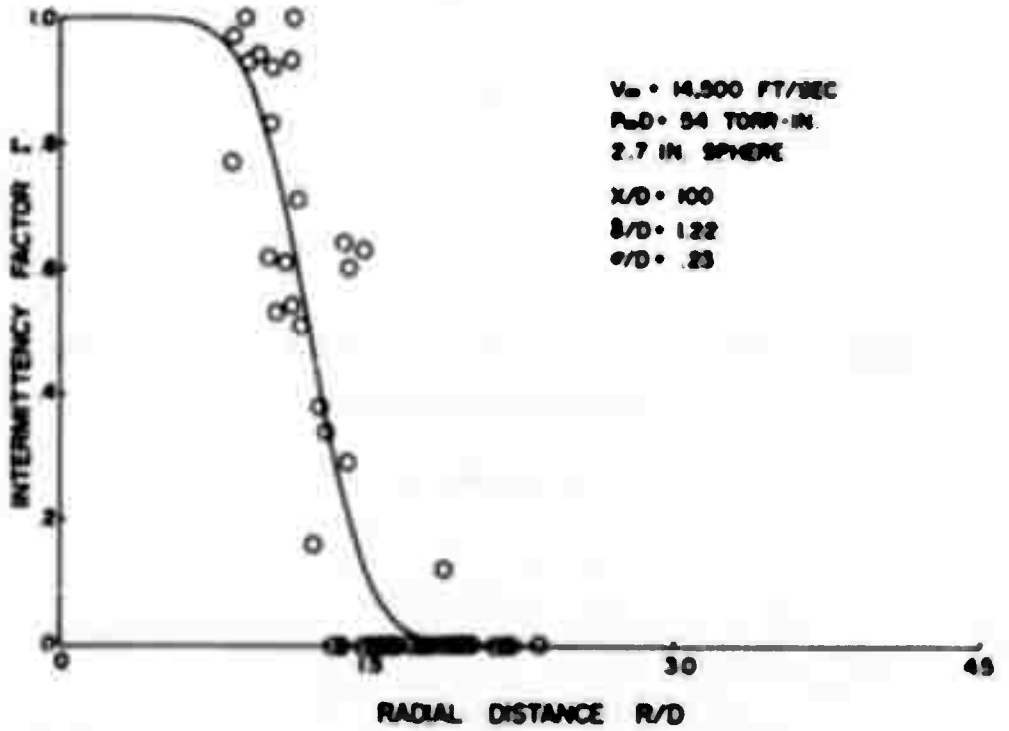

FIGURE 4b

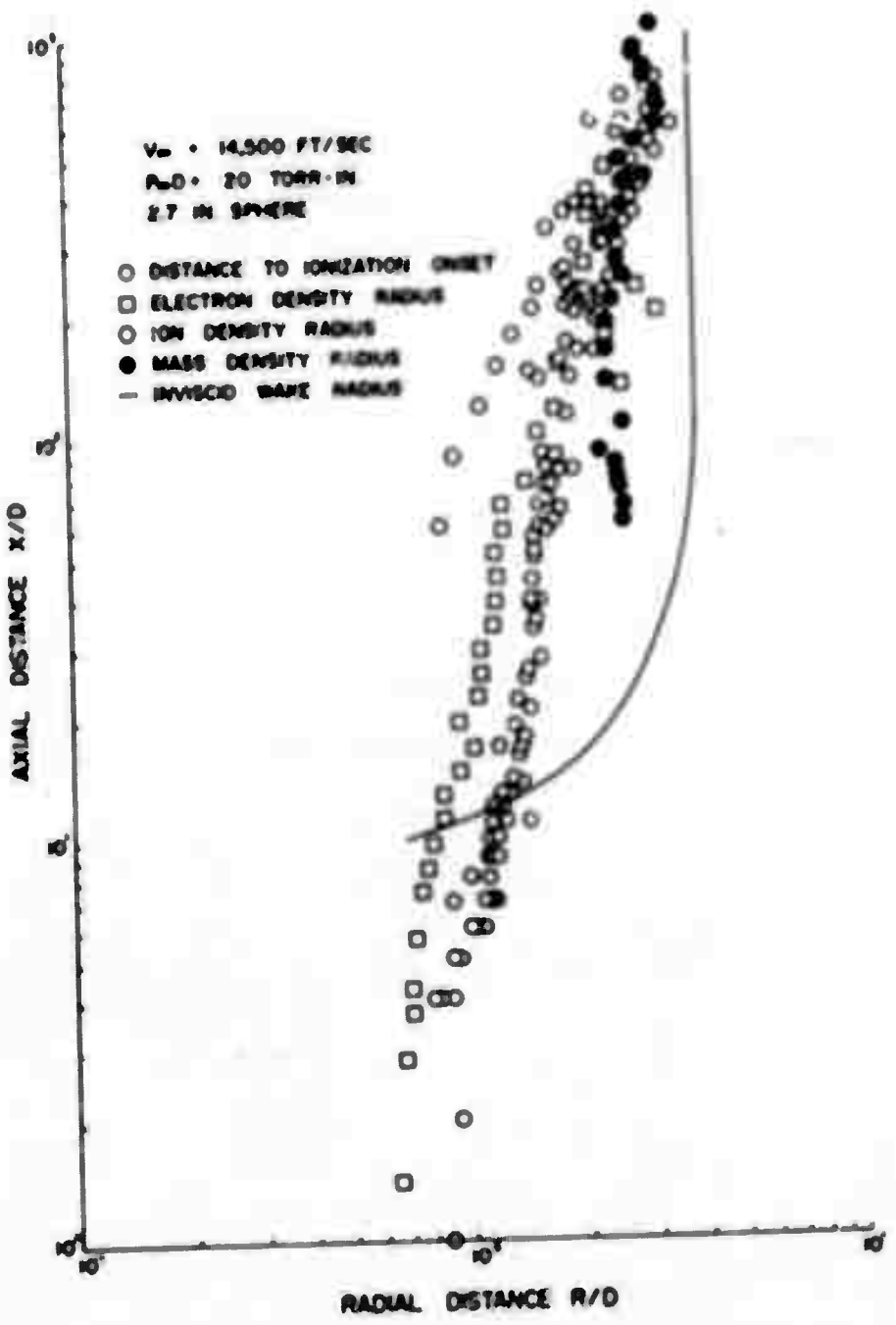
V∞ = 14,500 FT/SEC
P∞D = 20 TORR-IN
2.7 IN SPHERE
DISTANCE TO IONIZATION ONSET
ELECTRON DENSITY RADIUS
ION DENSITY RADIUS
MASS DENSITY RADIUS
INVISCID WAKE RADIUS
AXIAL DISTANCE X/D
RADIAL DISTANCE R/D

FIGURE 5a

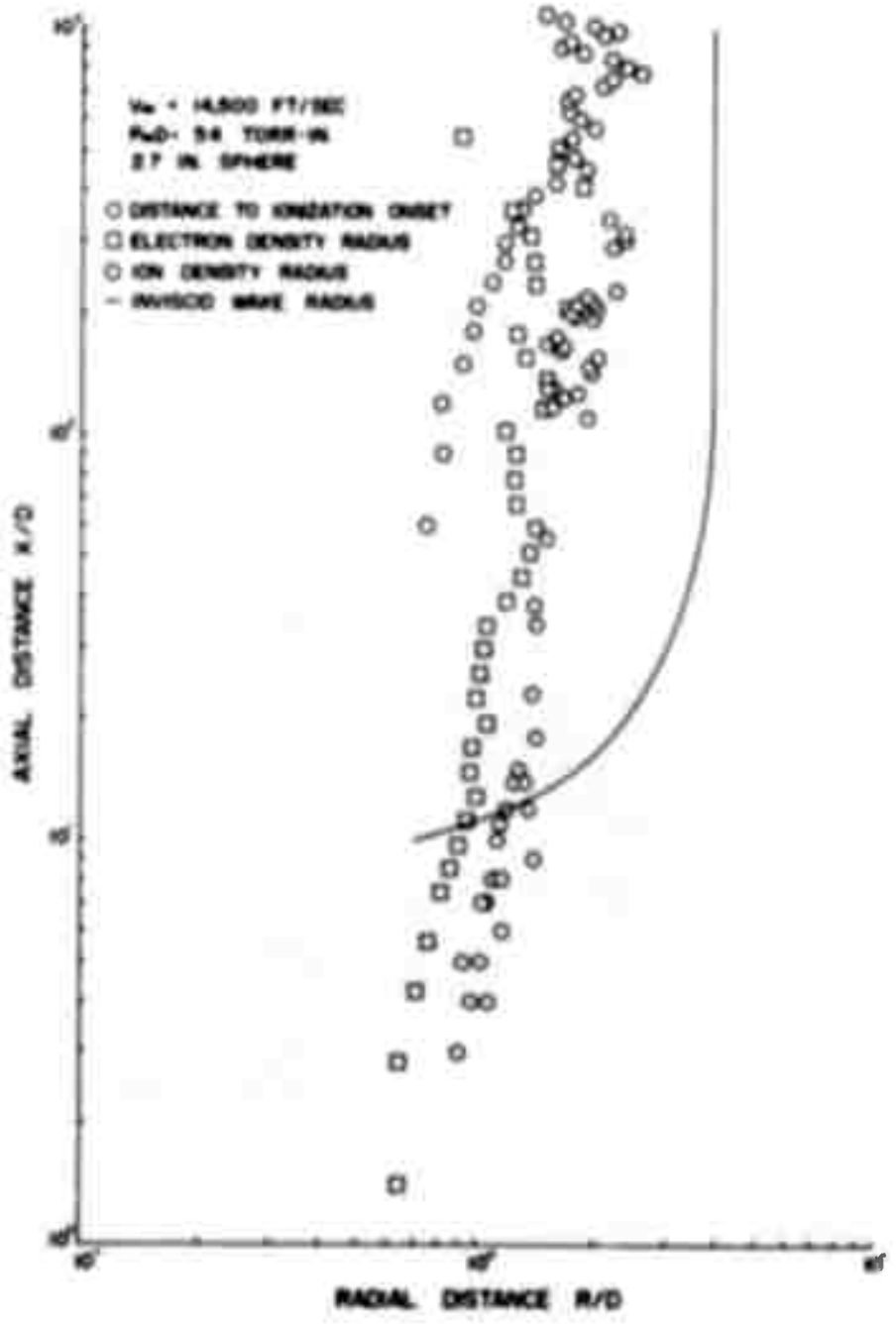
V∞ = 14,500 FT/SEC
P∞D= 54 TORR-IN
27 IN. SPHERE
DISTANCE TO IONIZATION ONSET
ELECTRON DENSITY RADIUS
ION DENSITY RADIUS
INVISCID SHOCK RADIUS
AXIAL DISTANCE X/D
RADIAL DISTANCE R/D

FIGURE 5b

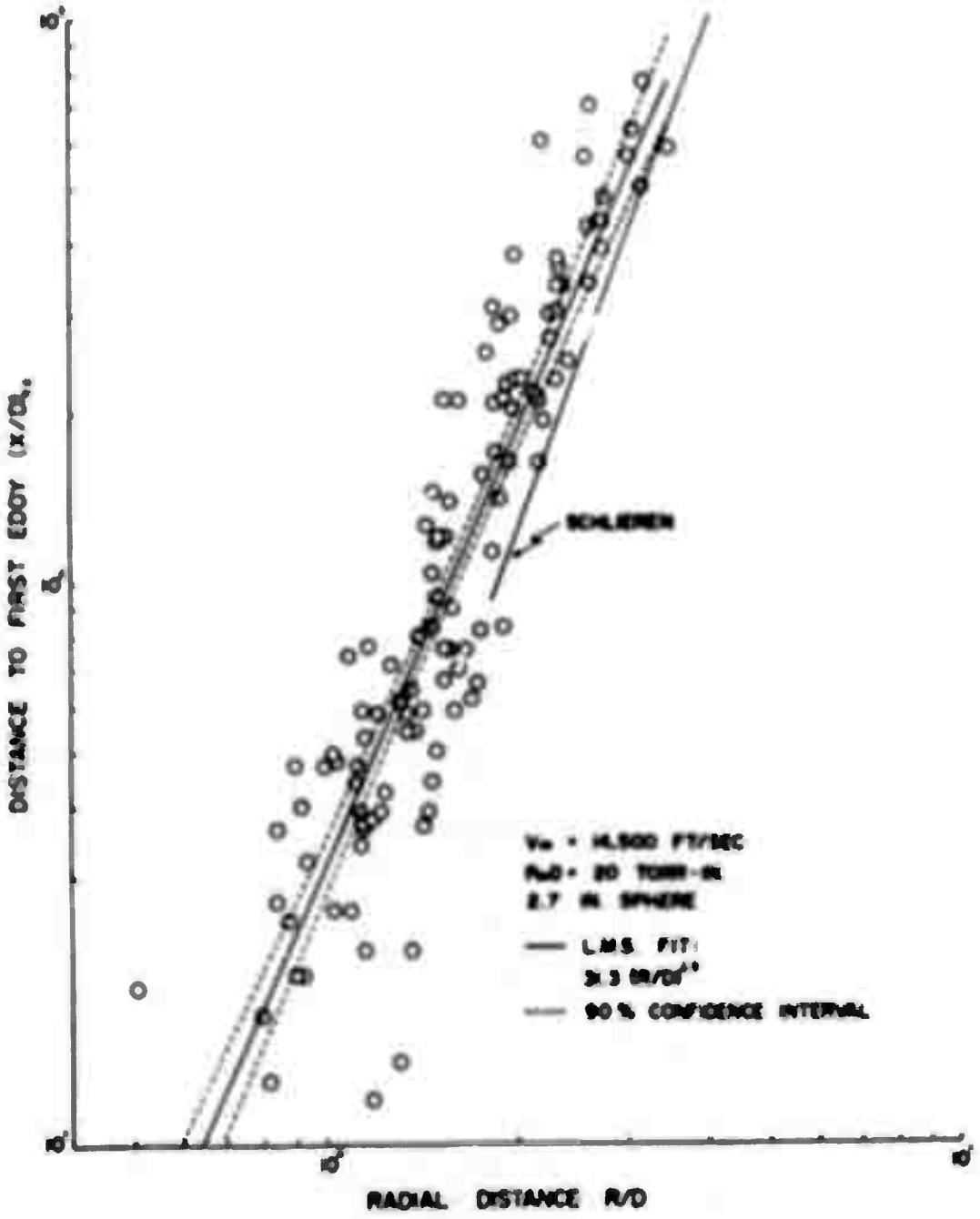
DISTANCE TO FIRST EDDY (X/DL)
RADIAL DISTANCE R/D
SCHLIEREN
LMS FIT
90 % CONFIDENCE INTERVAL

FIGURE 6a

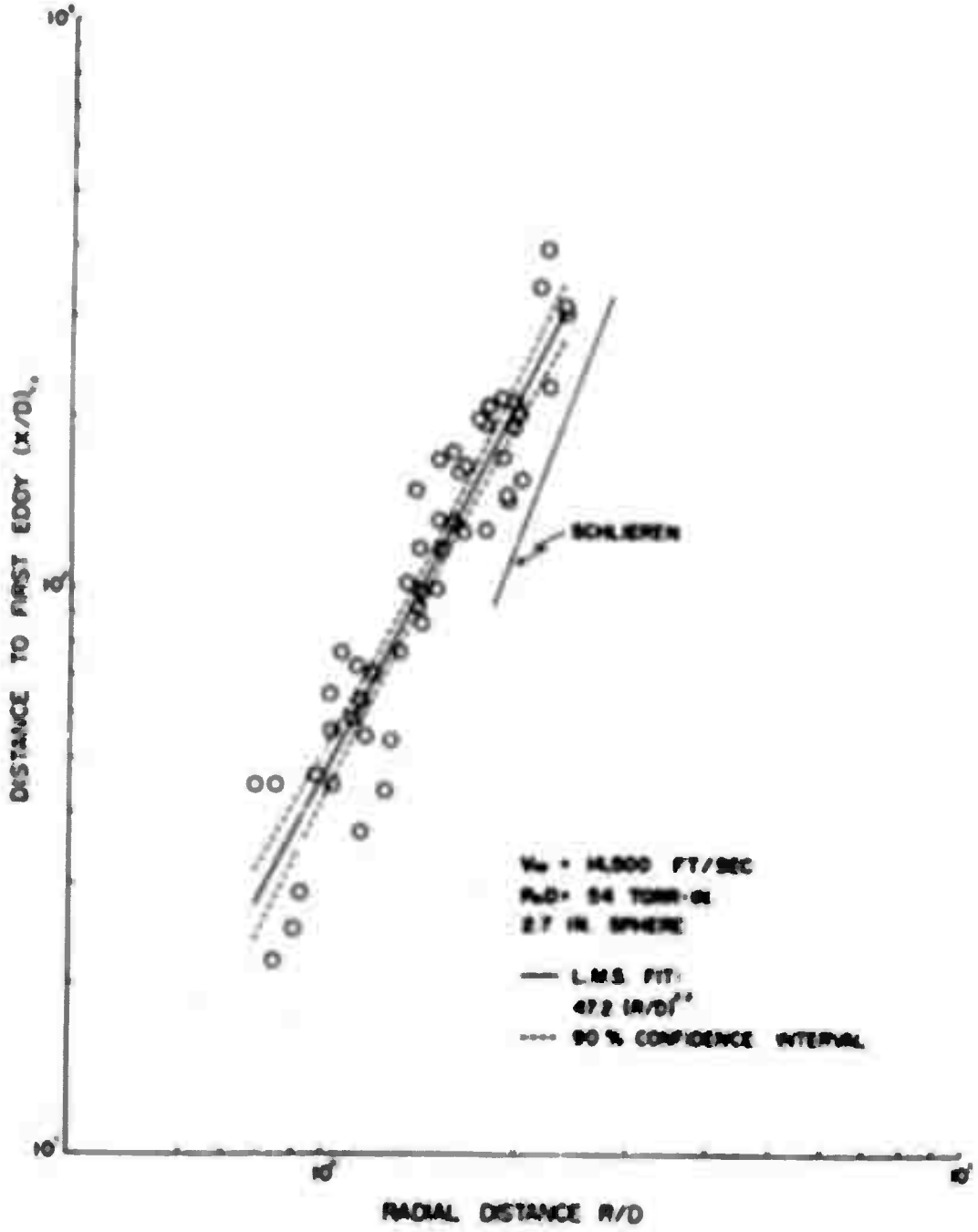
DISTANCE TO FIRST EDDY (X/D)$_e$
RADIAL DISTANCE R/D
SCHLIEREN
L.M.S. FIT:
90 % CONFIDENCE INTERVAL

FIGURE 6b

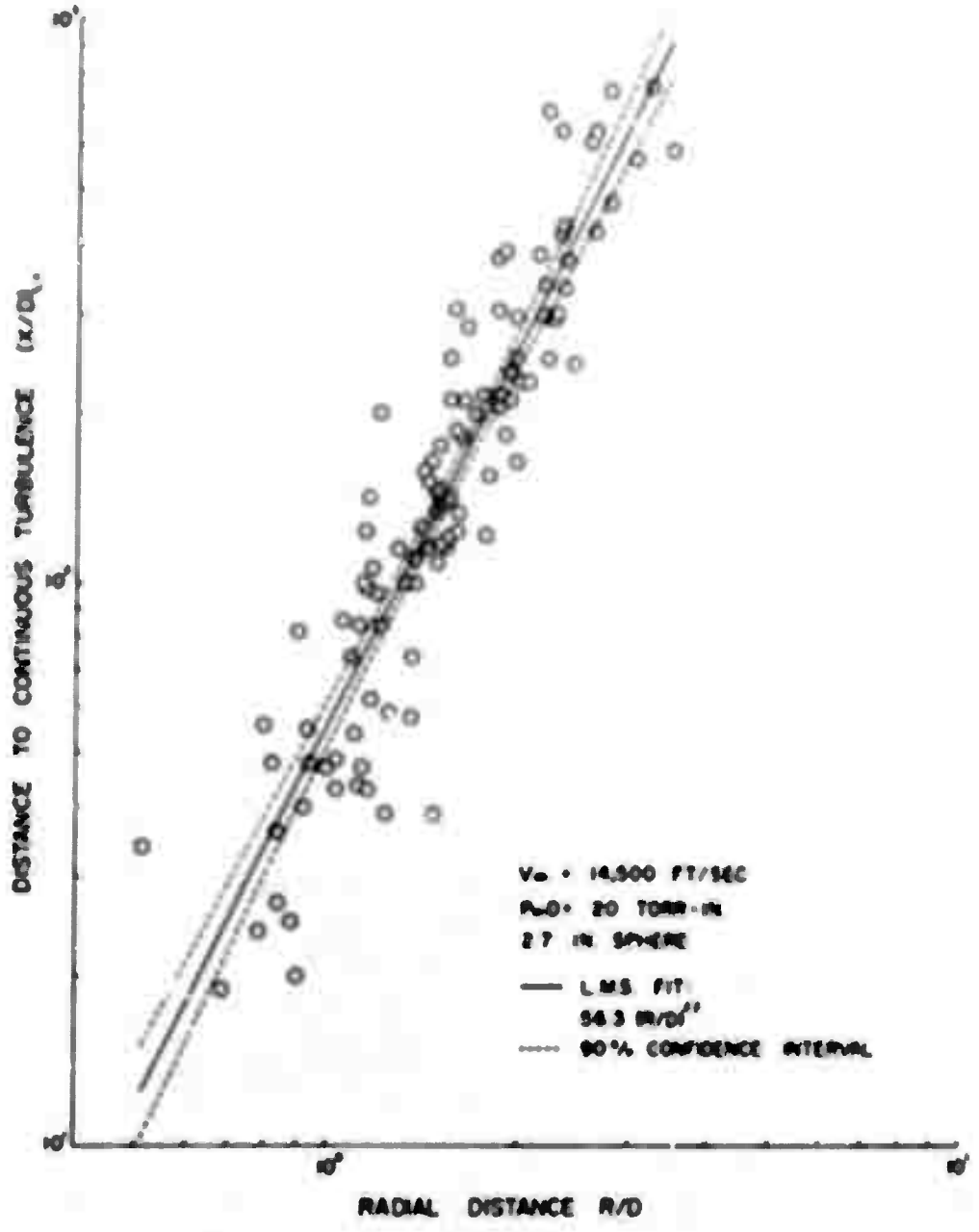
DISTANCE TO CONTINUOUS TURBULENCE (x/D)c
RADIAL DISTANCE R/D
LMS FIT
90% CONFIDENCE INTERVAL

FIGURE 7a

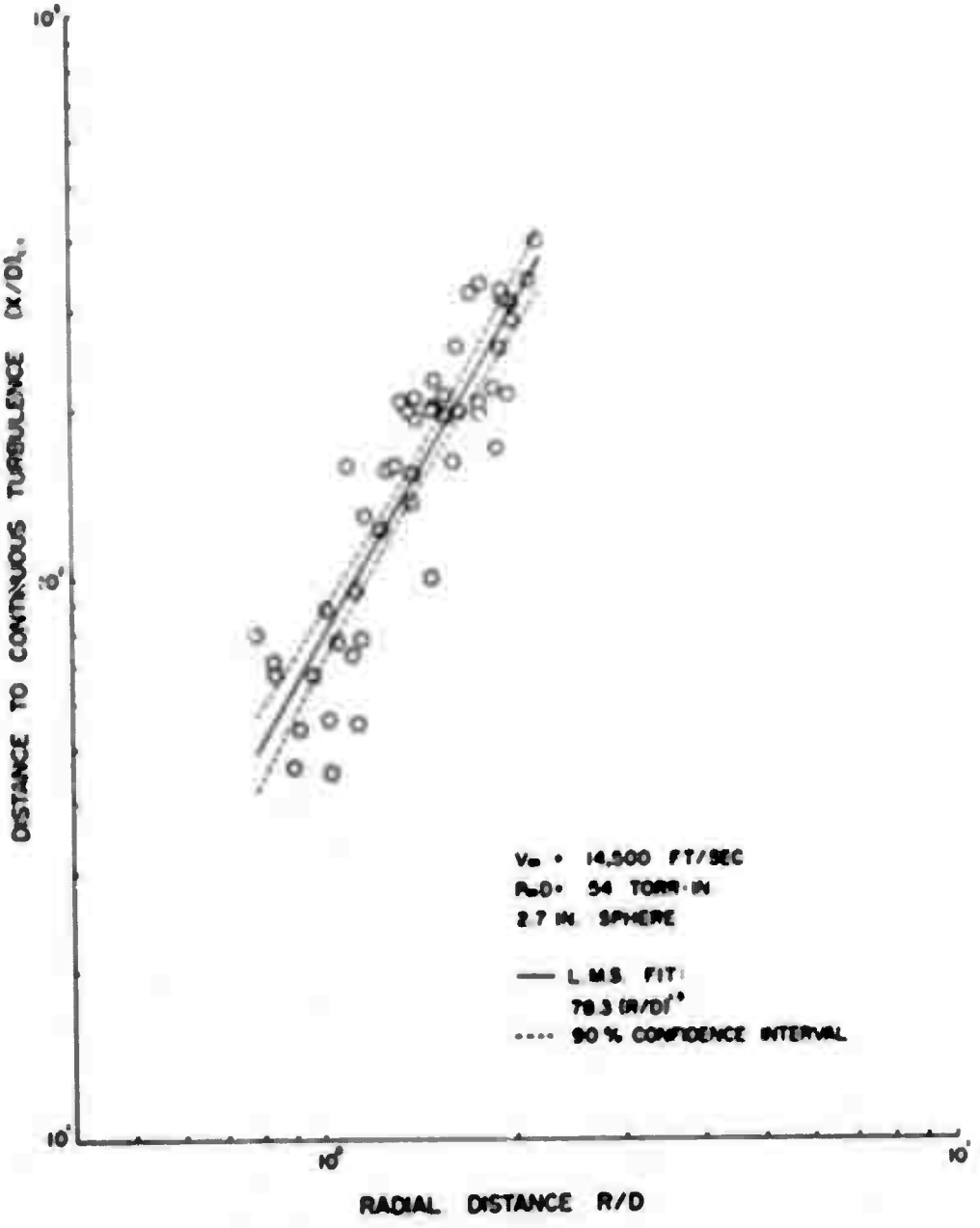
DISTANCE TO CONTINUOUS TURBULENCE (X/D)c
RADIAL DISTANCE R/D
V∞ = 14,500 FT/SEC
P∞D = 54 TORR-IN
2.7 IN. SPHERE
L.M.S. FIT:
78.3 (R/D)^1.9
90 % CONFIDENCE INTERVAL

FIGURE 7b

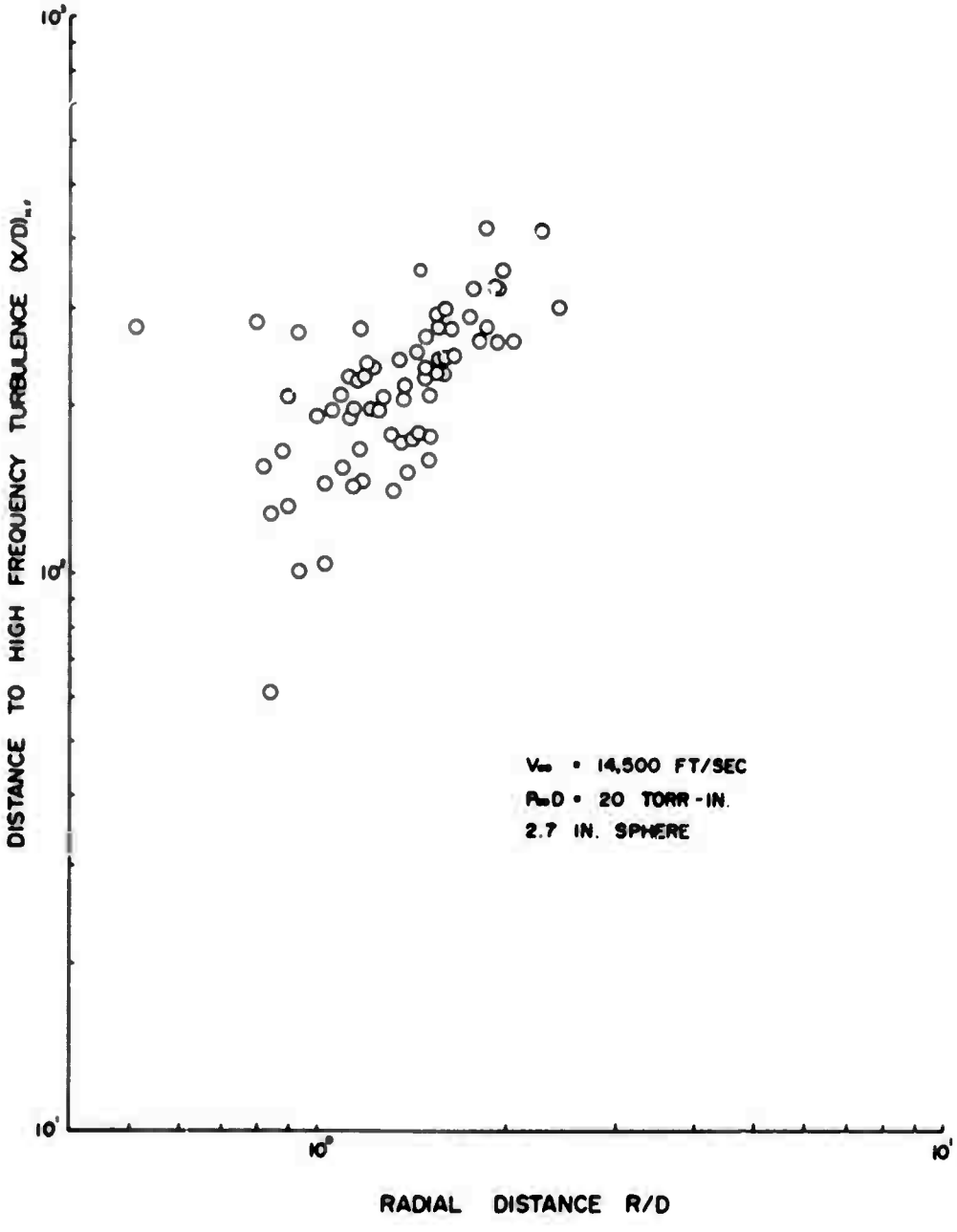
DISTANCE TO HIGH FREQUENCY TURBULENCE (X/D)∞
10³
10²
10¹
10⁰
10¹
V∞ • 14,500 FT/SEC
P∞D • 20 TORR-IN.
2.7 IN. SPHERE
RADIAL DISTANCE R/D

FIGURE 8

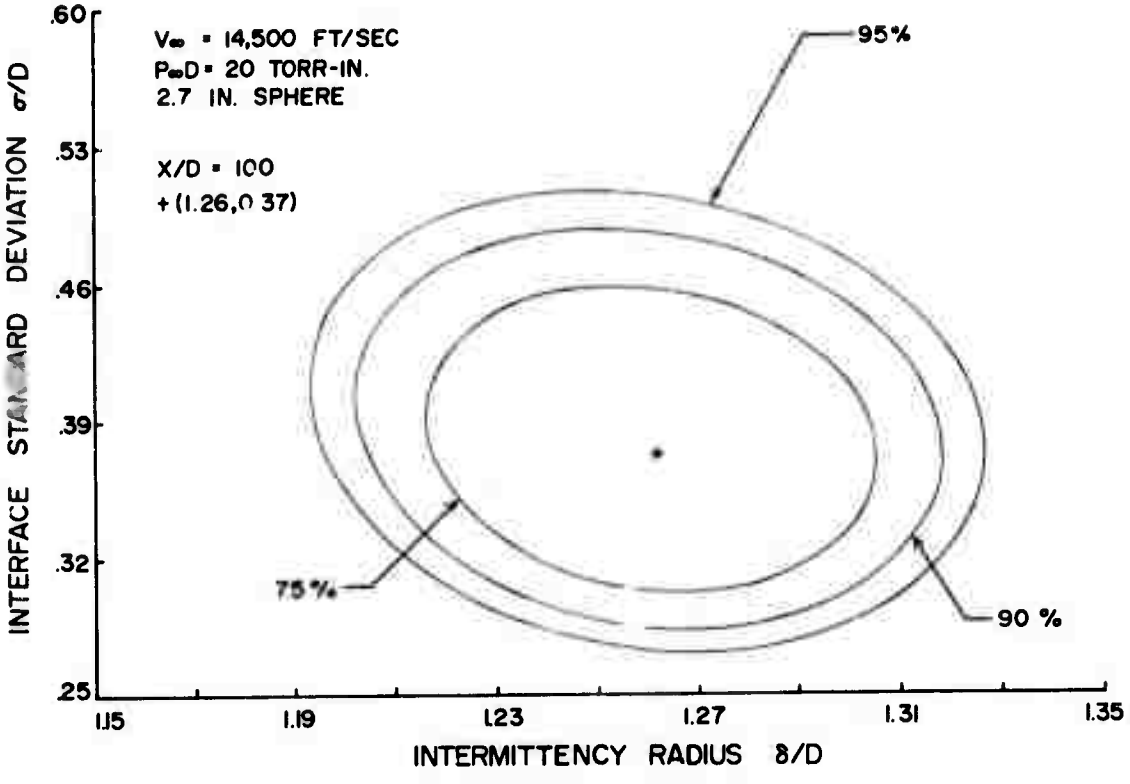

FIGURE 9

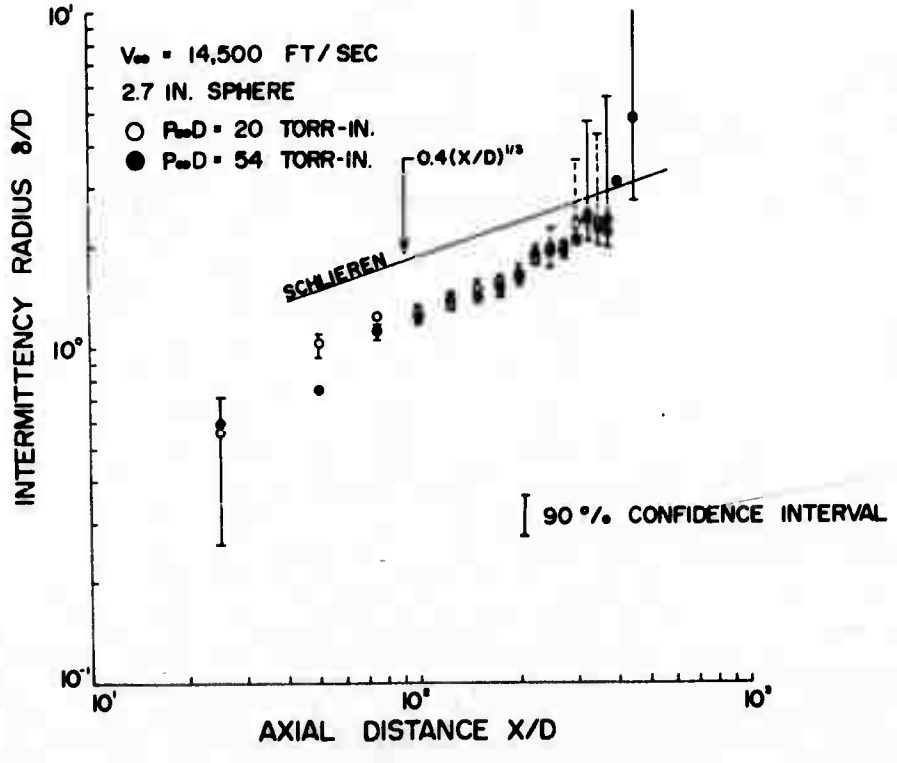

FIGURE 10

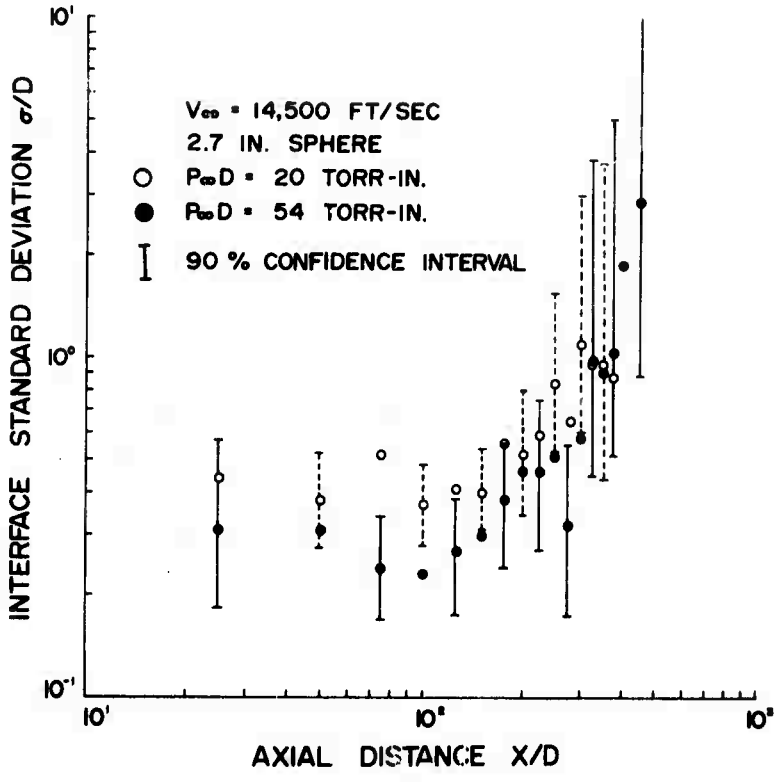

FIGURE 11

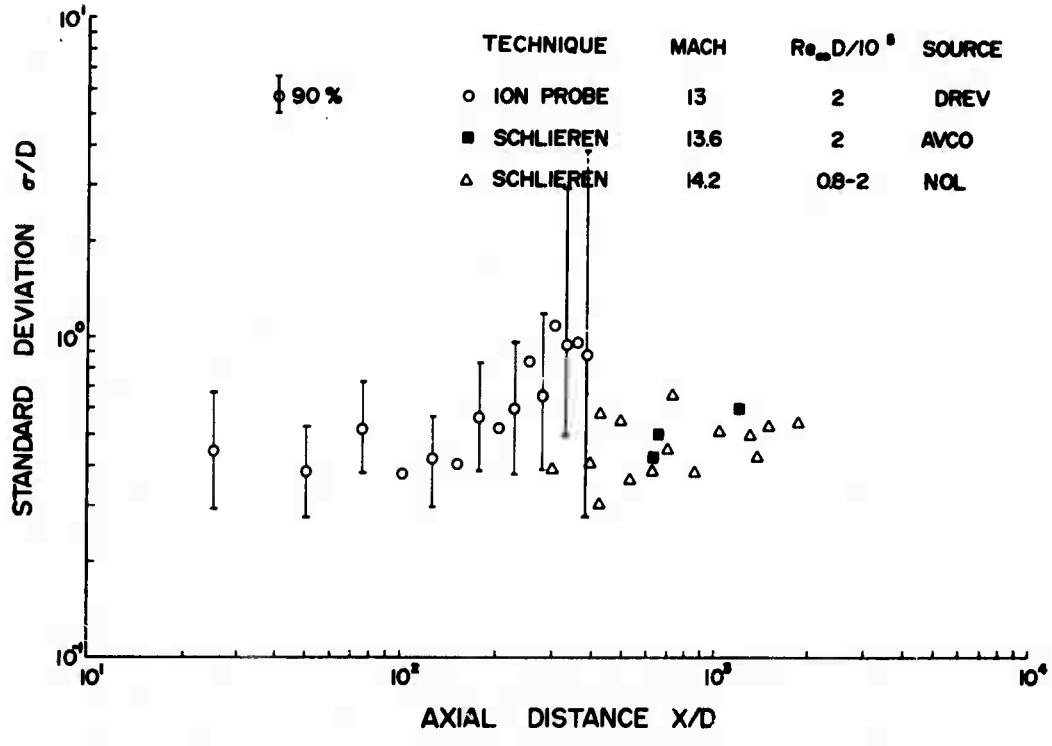

FIGURE 12

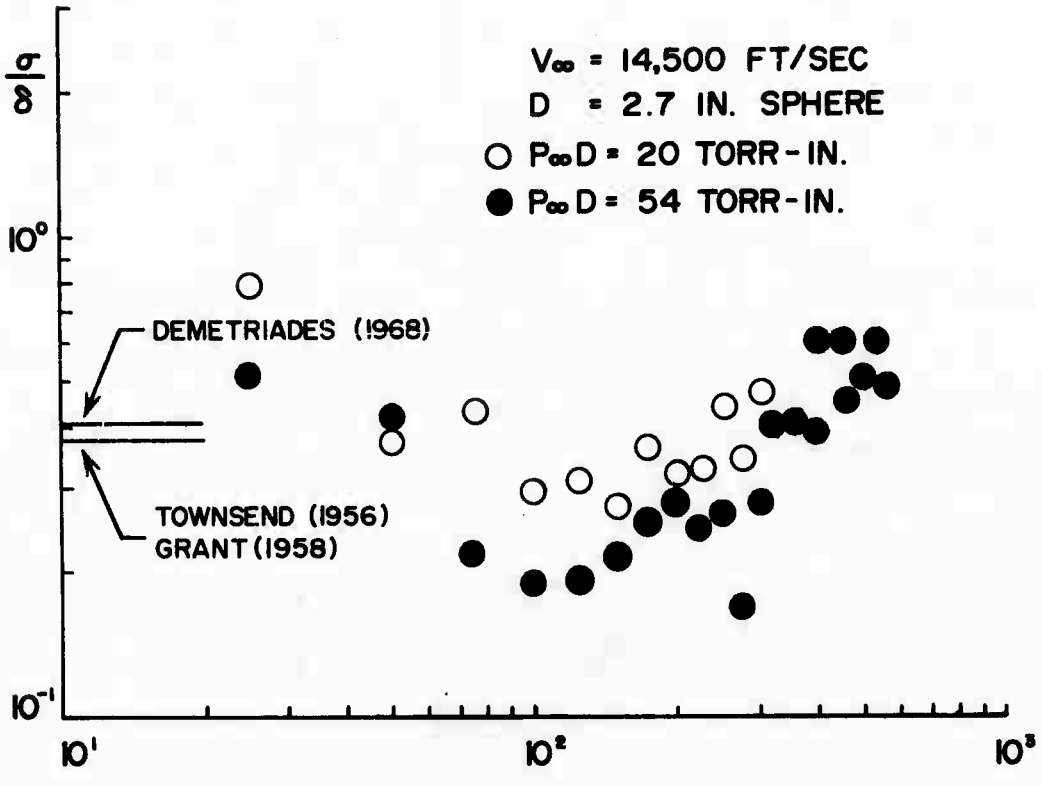
V_∞ = 14,500 FT/SEC
D = 2.7 IN. SPHERE
○ $P_\infty D$ = 20 TORR-IN.
● $P_\infty D$ = 54 TORR-IN.
$\frac{\sigma}{\delta}$
10^0
10^{-1}
DEMETRIADES (1968)
TOWNSEND (1956)
GRANT (1958)
10^1
10^2
10^3
AXIAL DISTANCE X/D

FIGURE 13

APPENDIX A

RADIAL DISTRIBUTIONS OF INTERMITTENCY ESTIMATES

P_∞ = 7.6 TORR

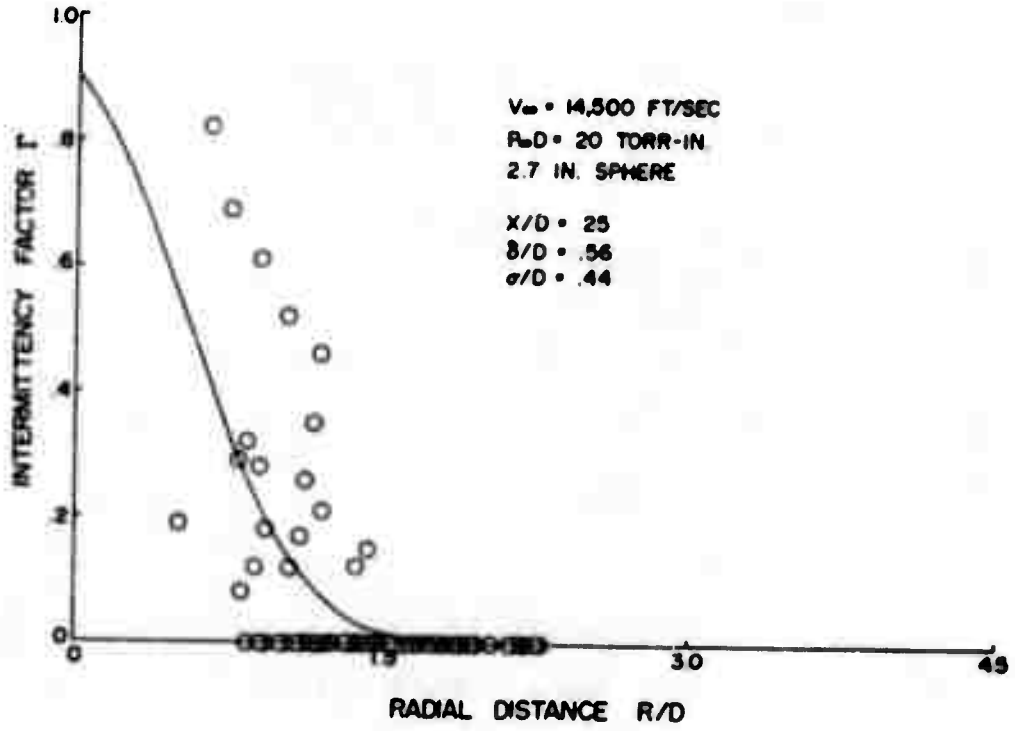

FIGURE A-1

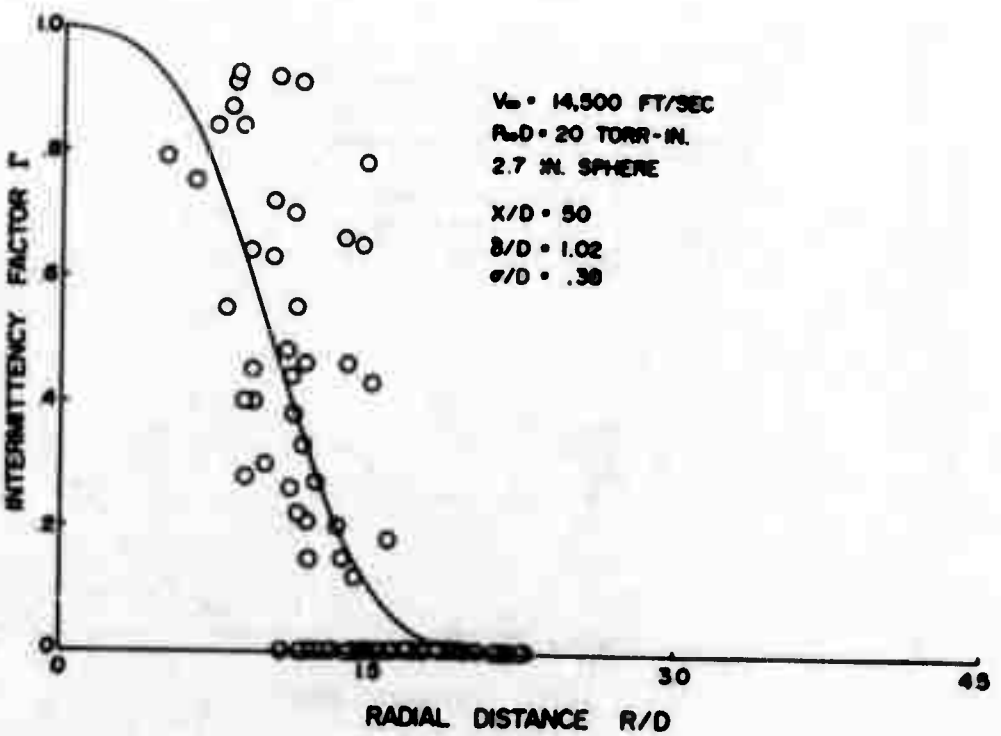

FIGURE A-2

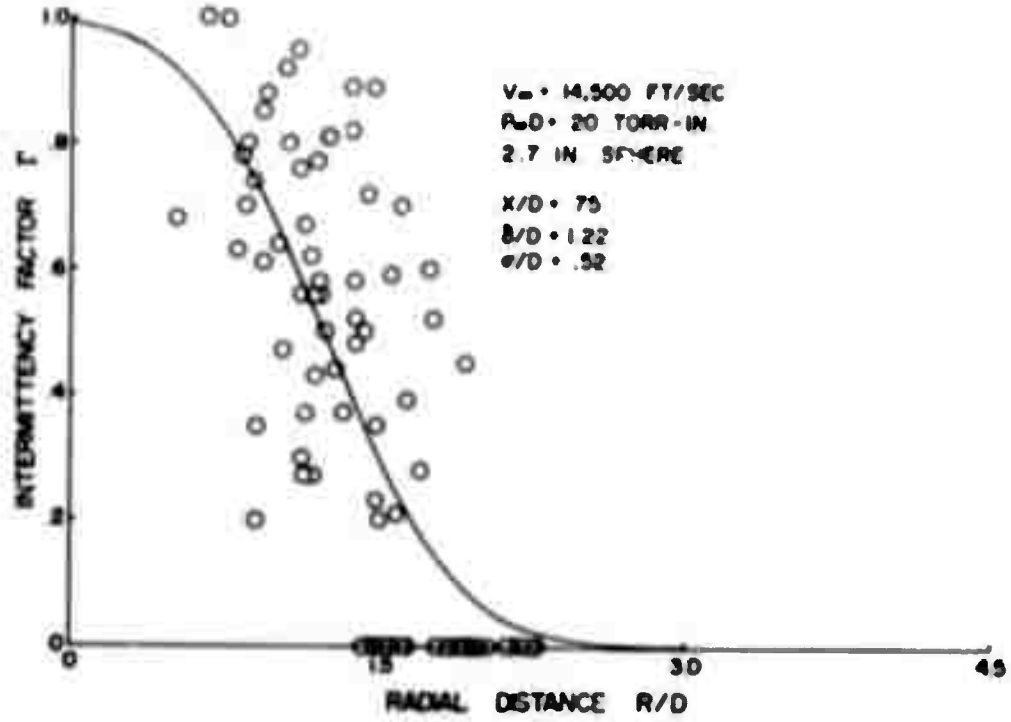

FIGURE A-3

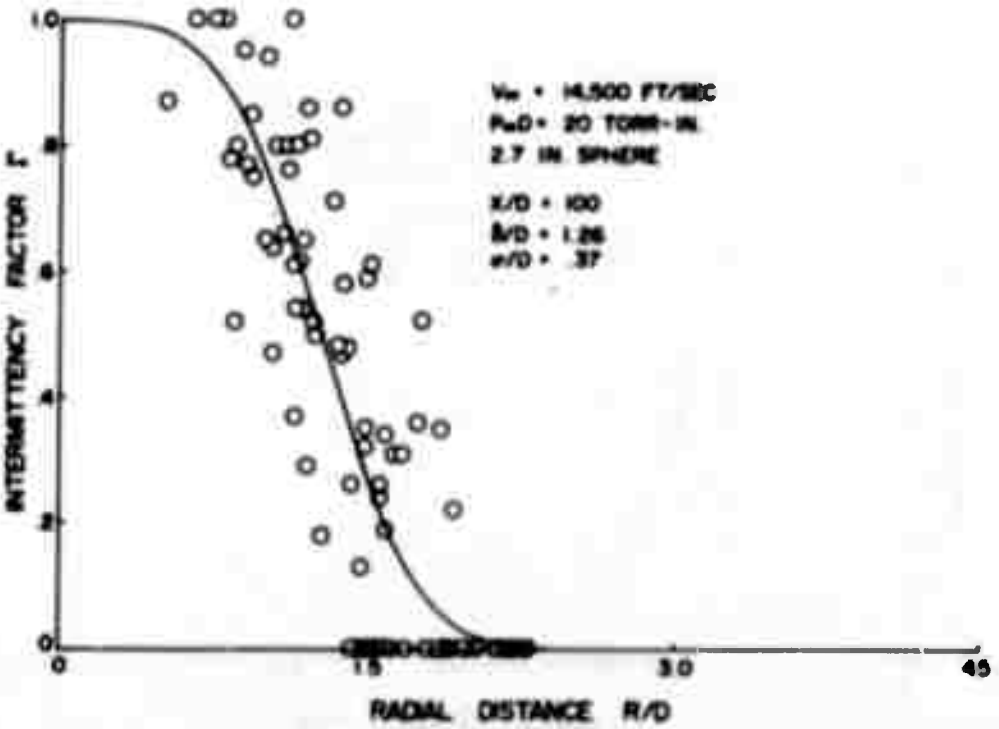

FIGURE A-4

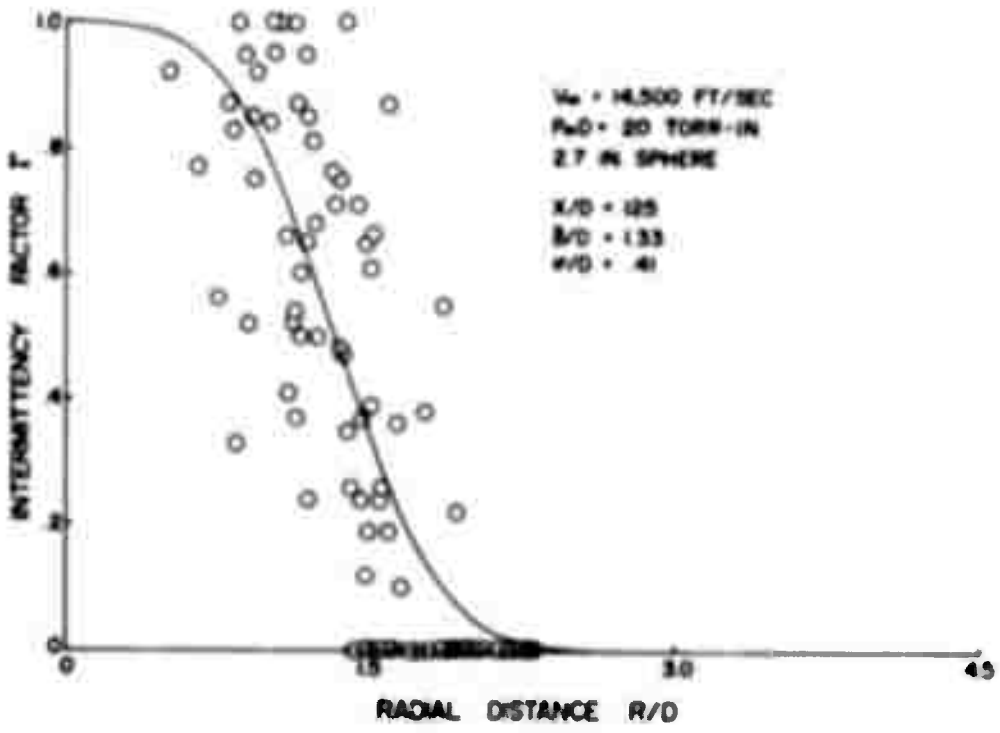

FIGURE A-5

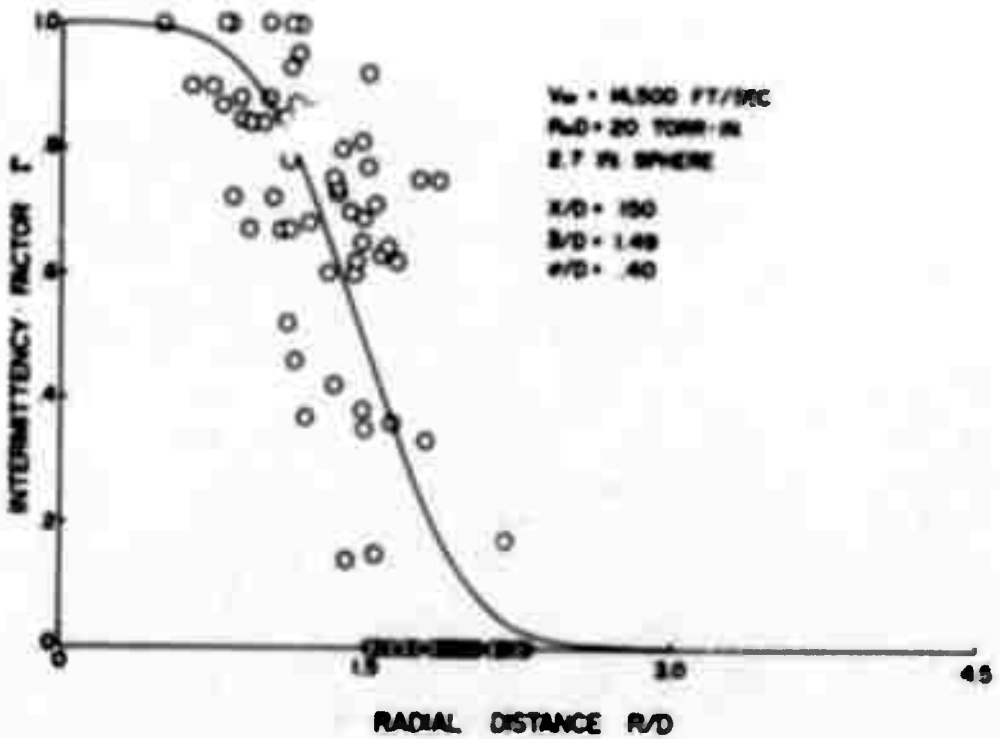

FIGURE A-6

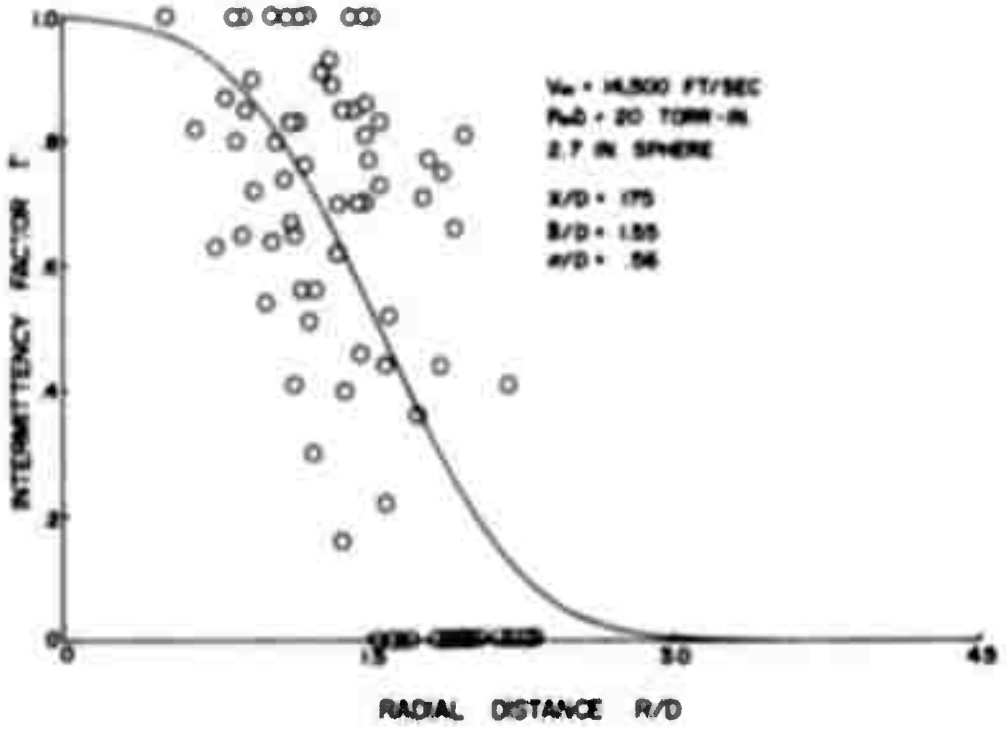

FIGURE A-7

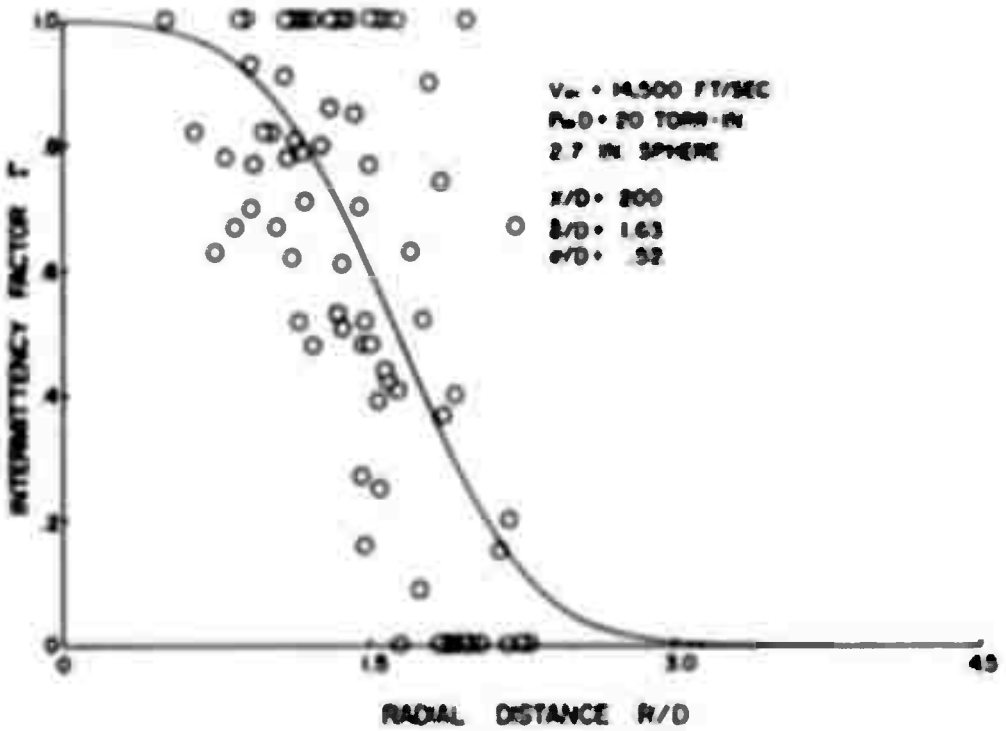

FIGURE A-8

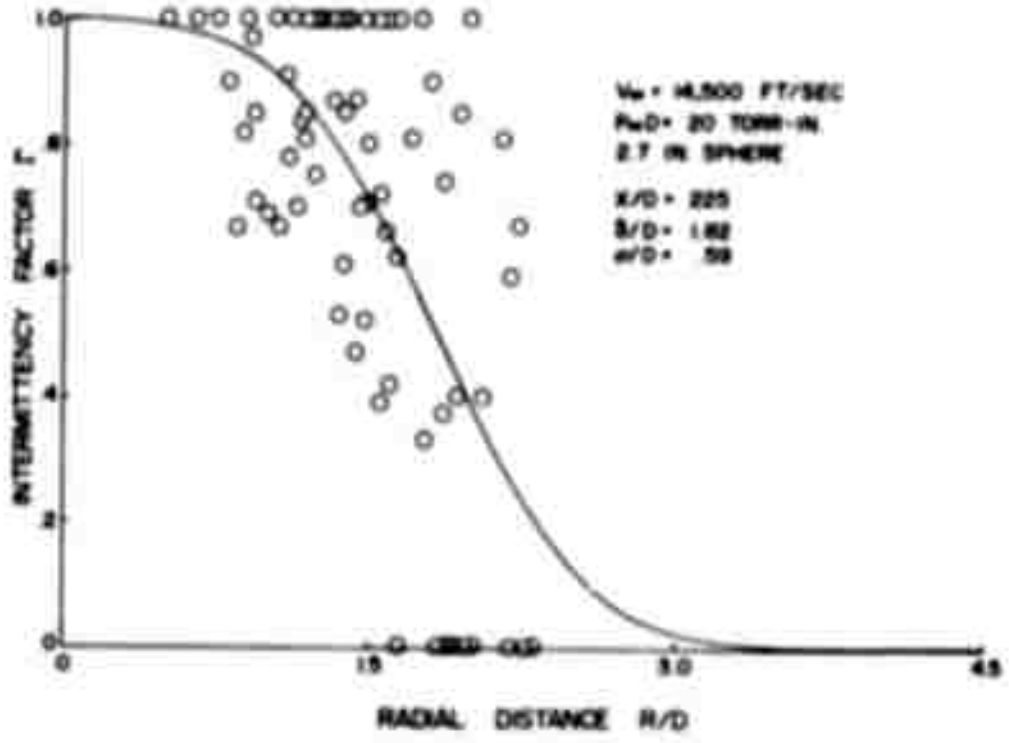

FIGURE A-9

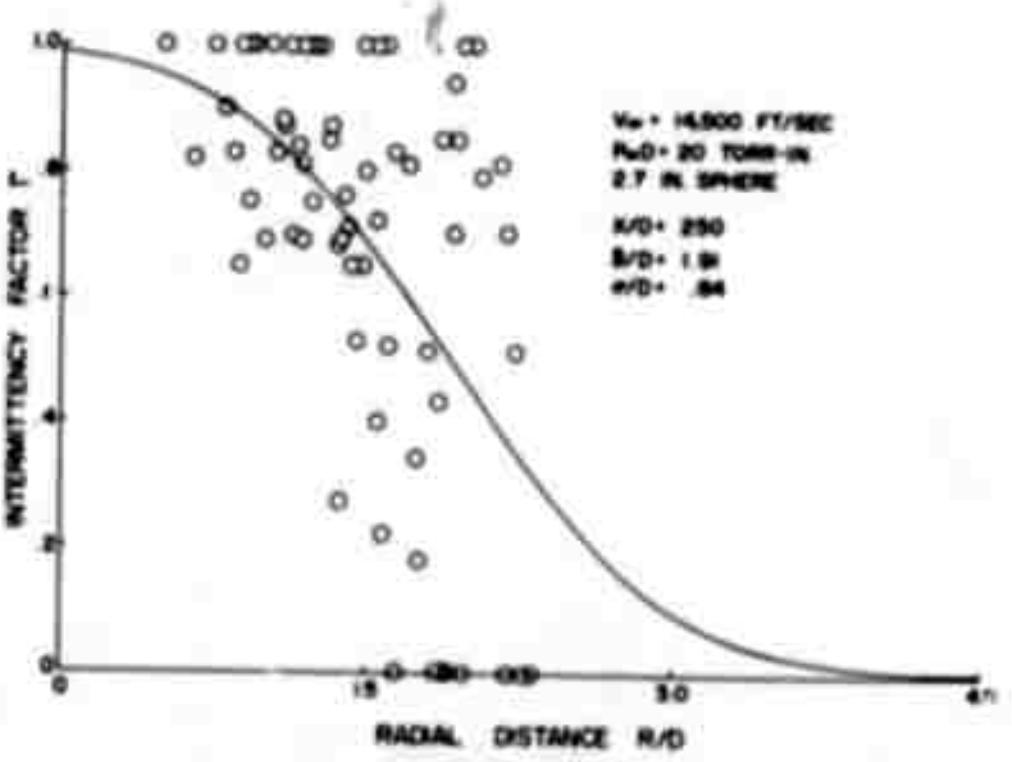

FIGURE A-10

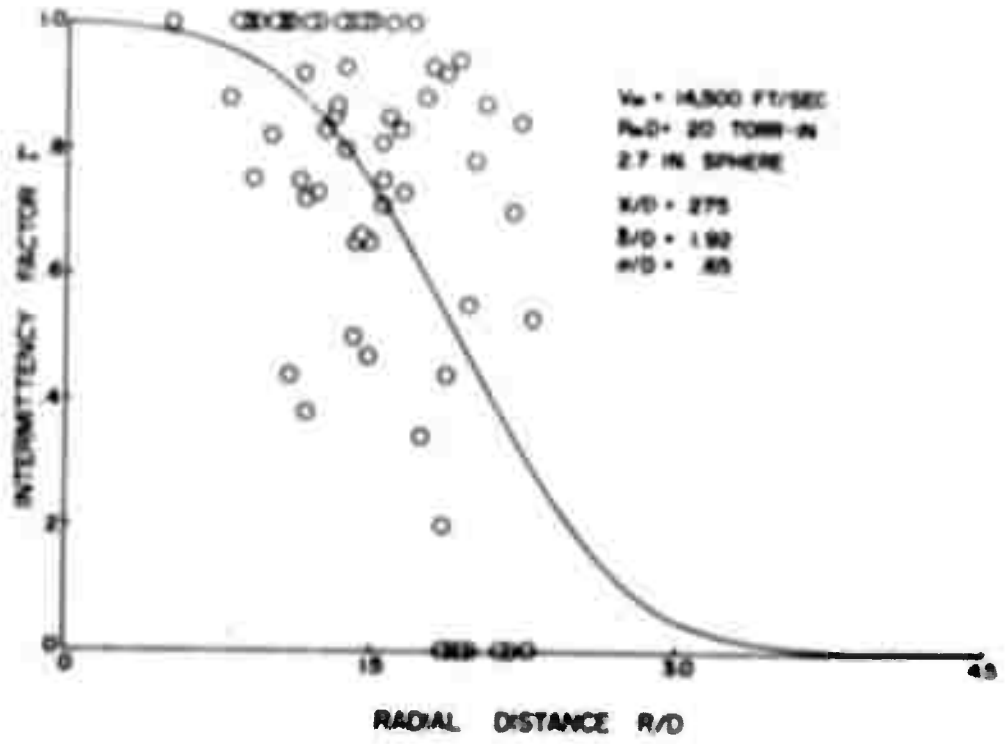

FIGURE A-11

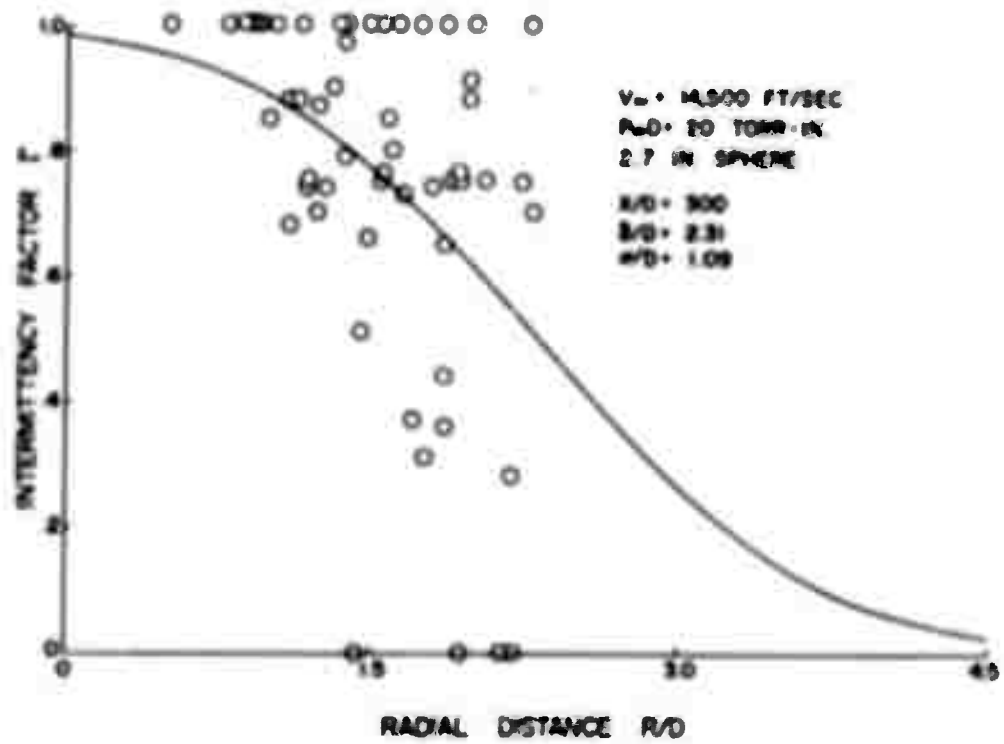

FIGURE A-12

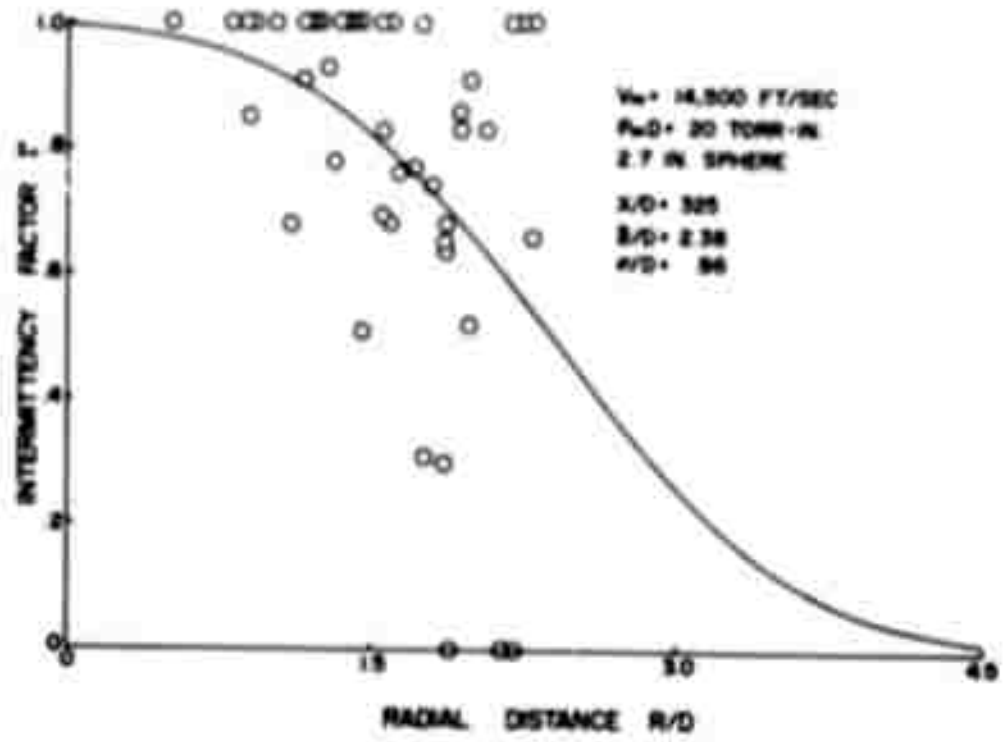

FIGURE A-13

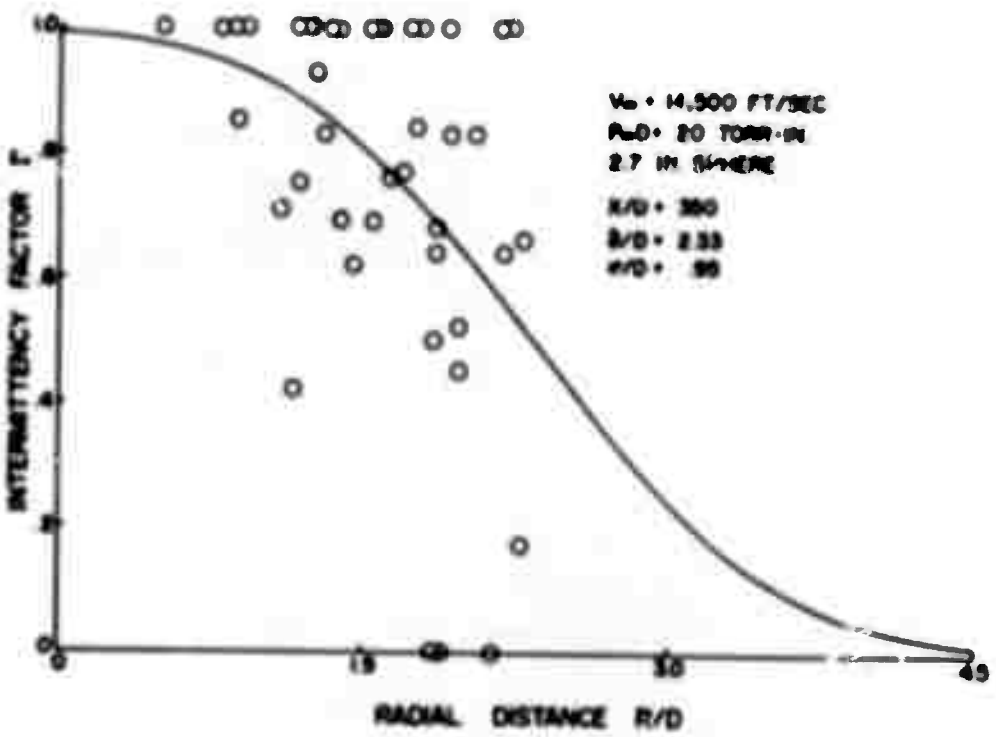

FIGURE A-14

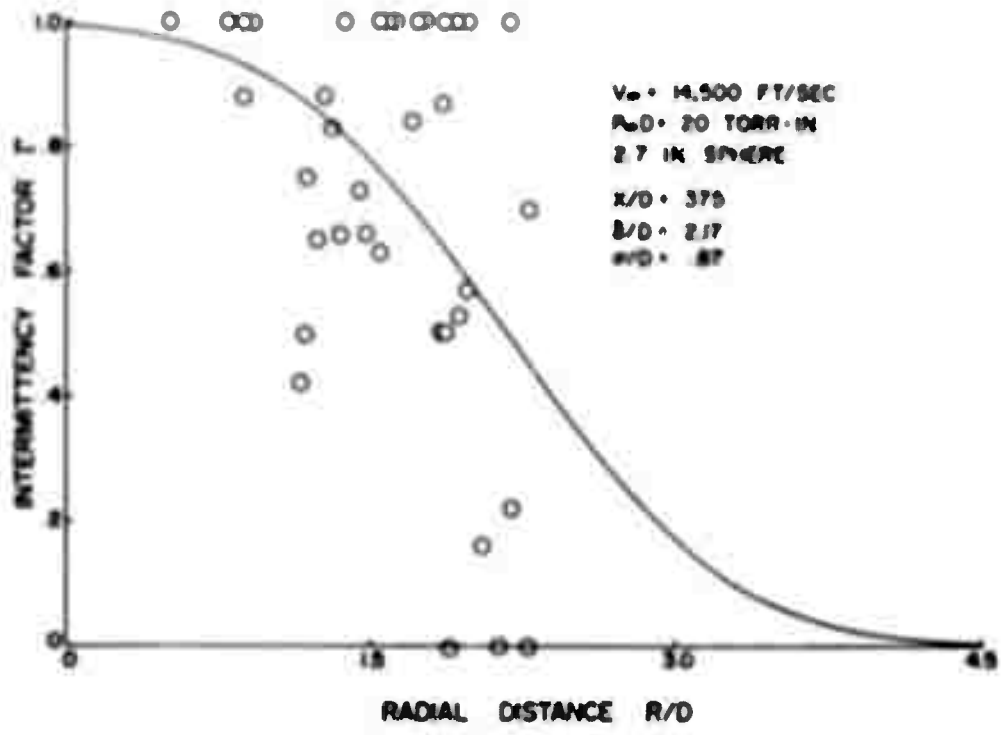

FIGURE A-15

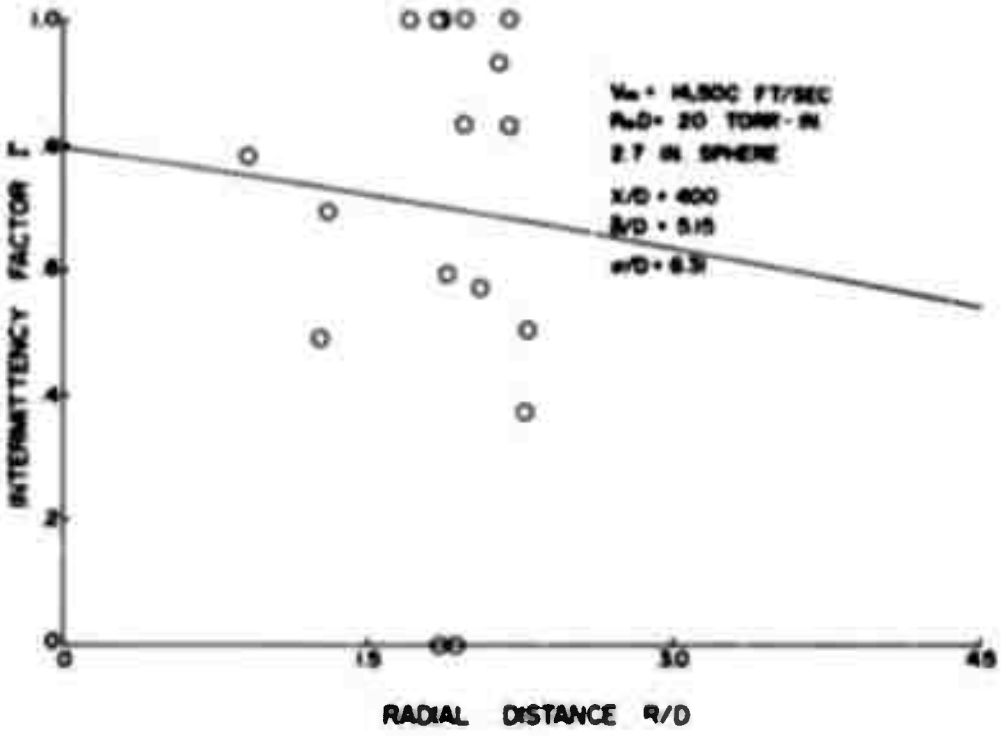

FIGURE A-16

APPENDIX B

RADIAL DISTRIBUTIONS OF INTERMITTENCY ESTIMATES

P_∞ = 20 TORR

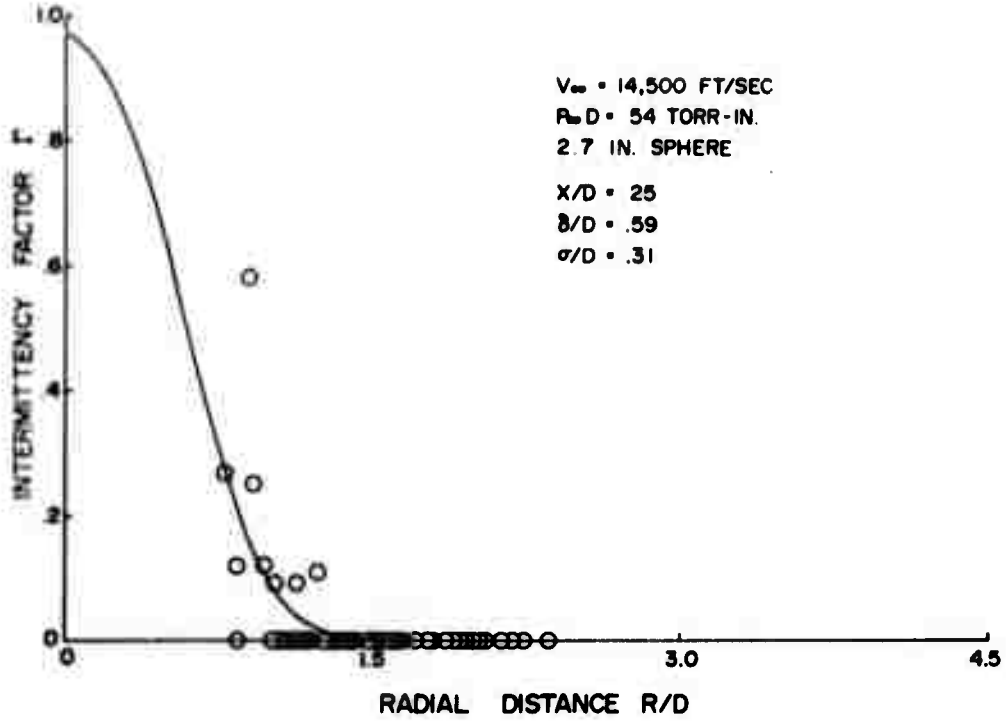

FIGURE B-1

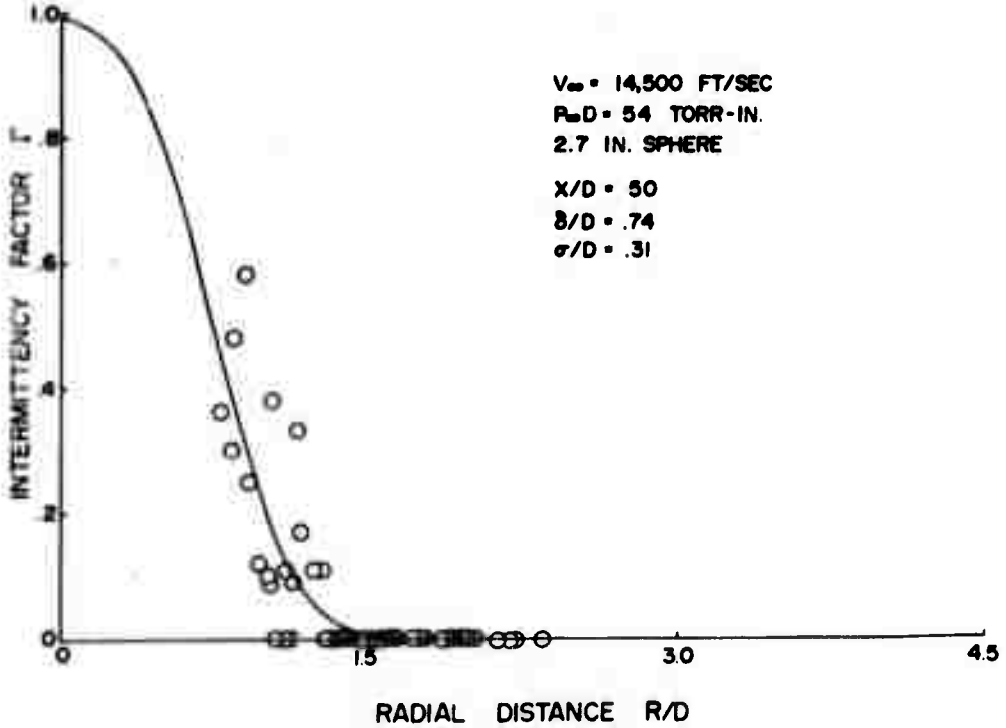

FIGURE B-2

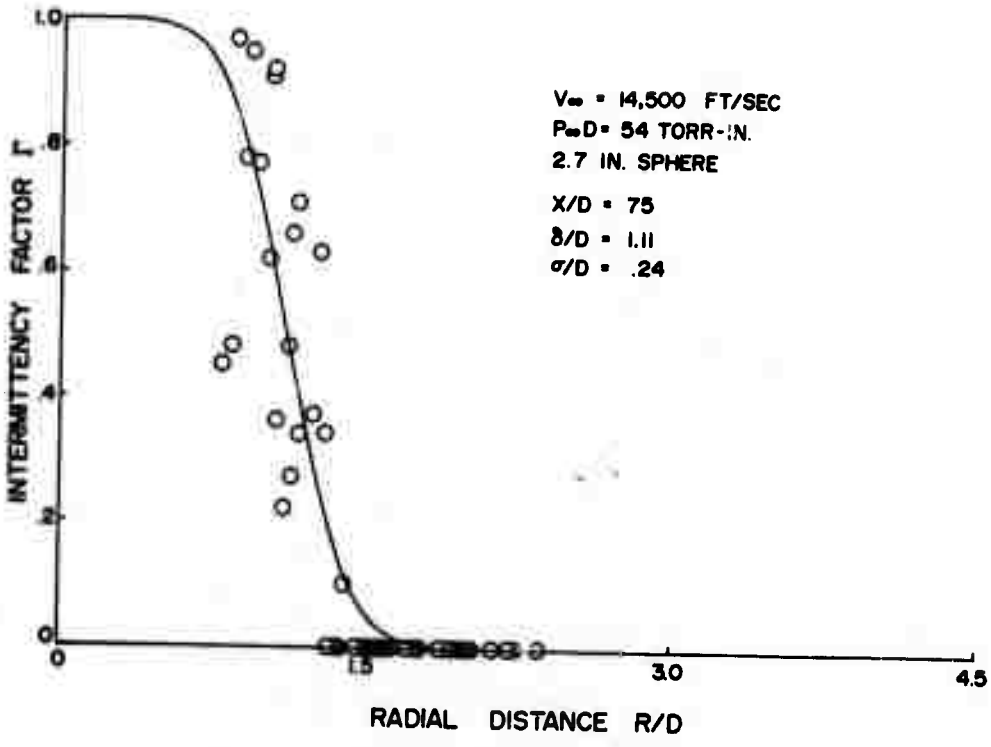

FIGURE B-3

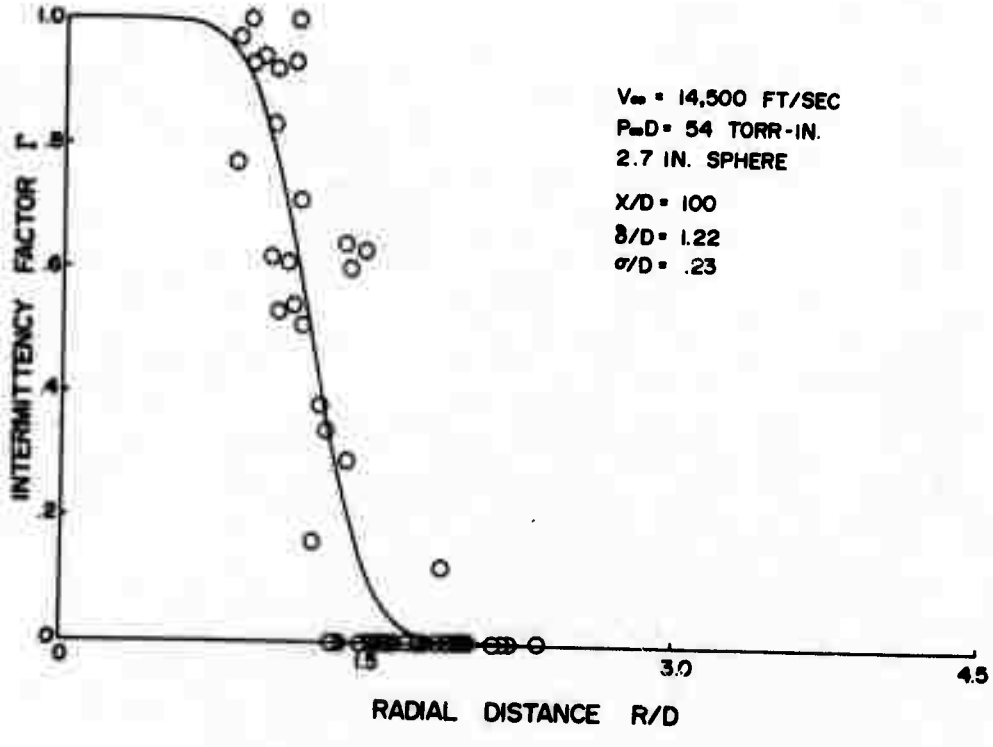

FIGURE B-4

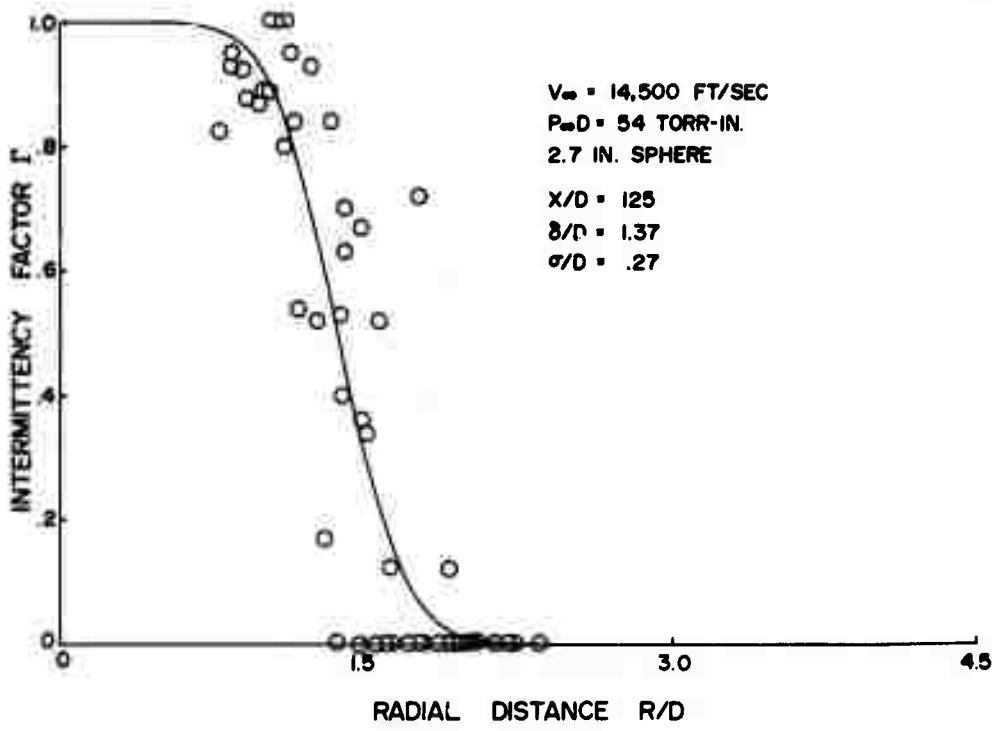

FIGURE B-5

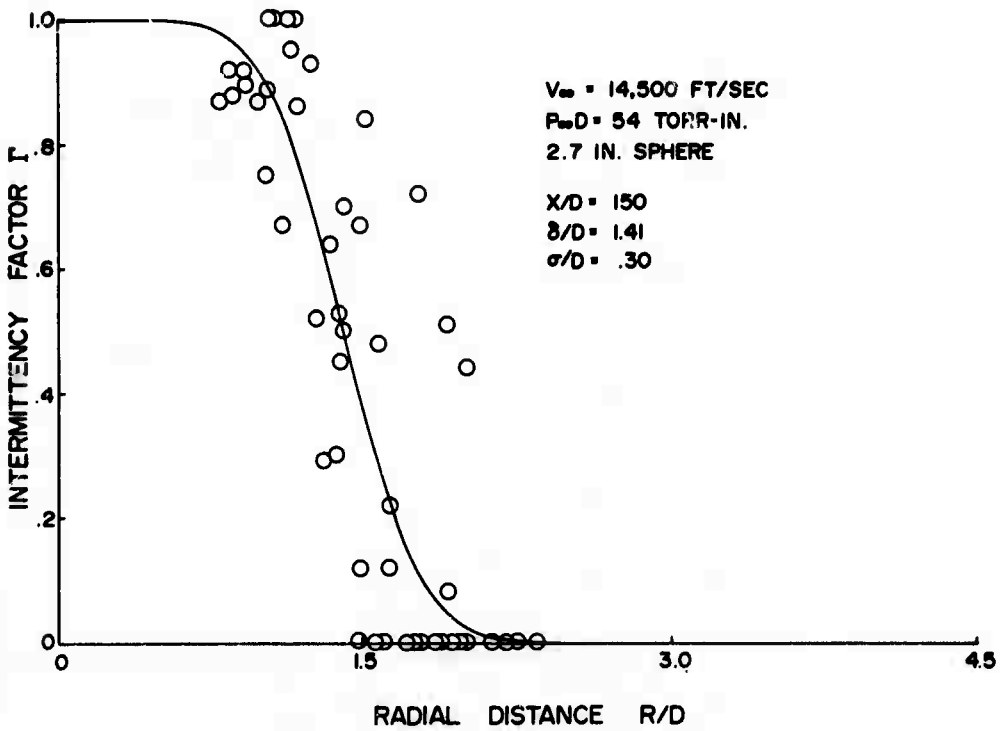

FIGURE B-6

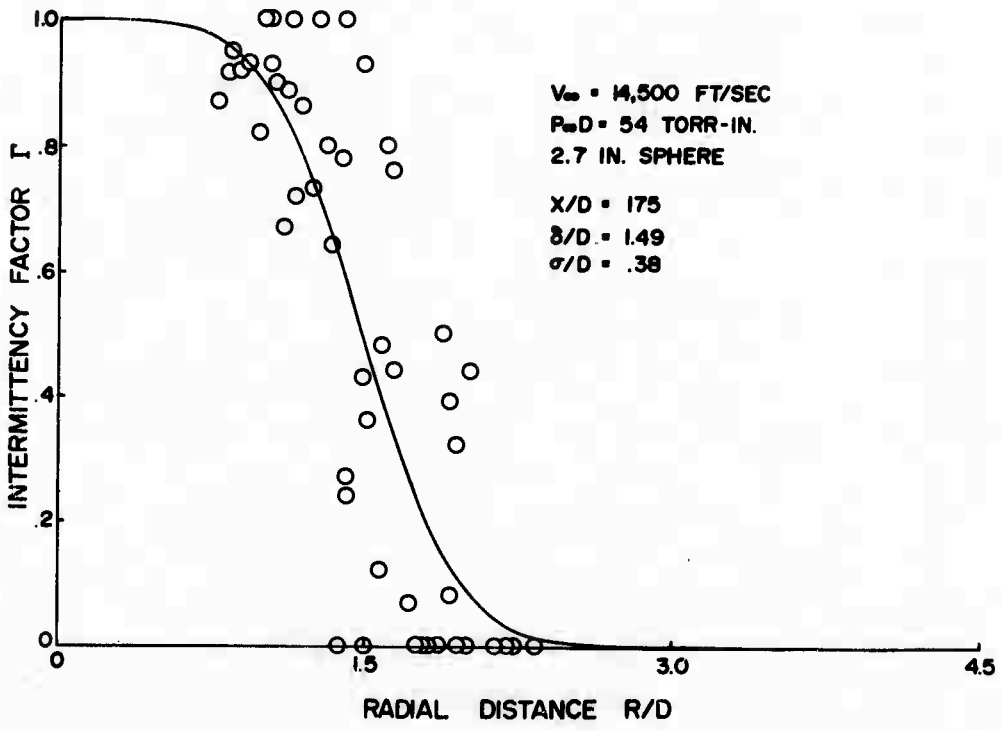

FIGURE B-7

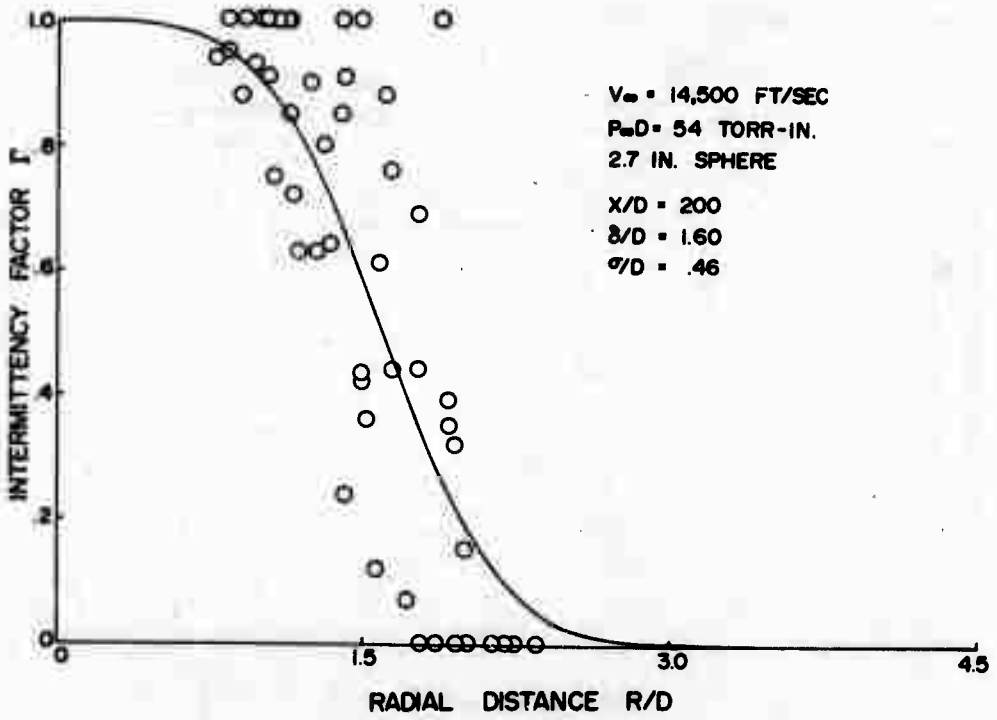

FIGURE B-8

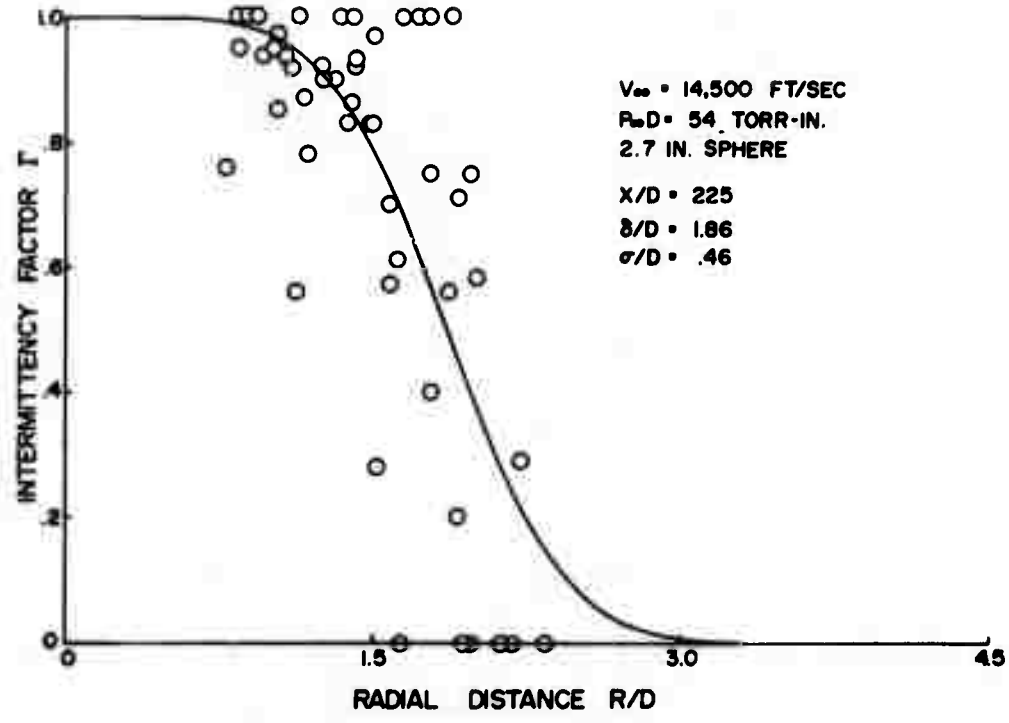

FIGURE B-9

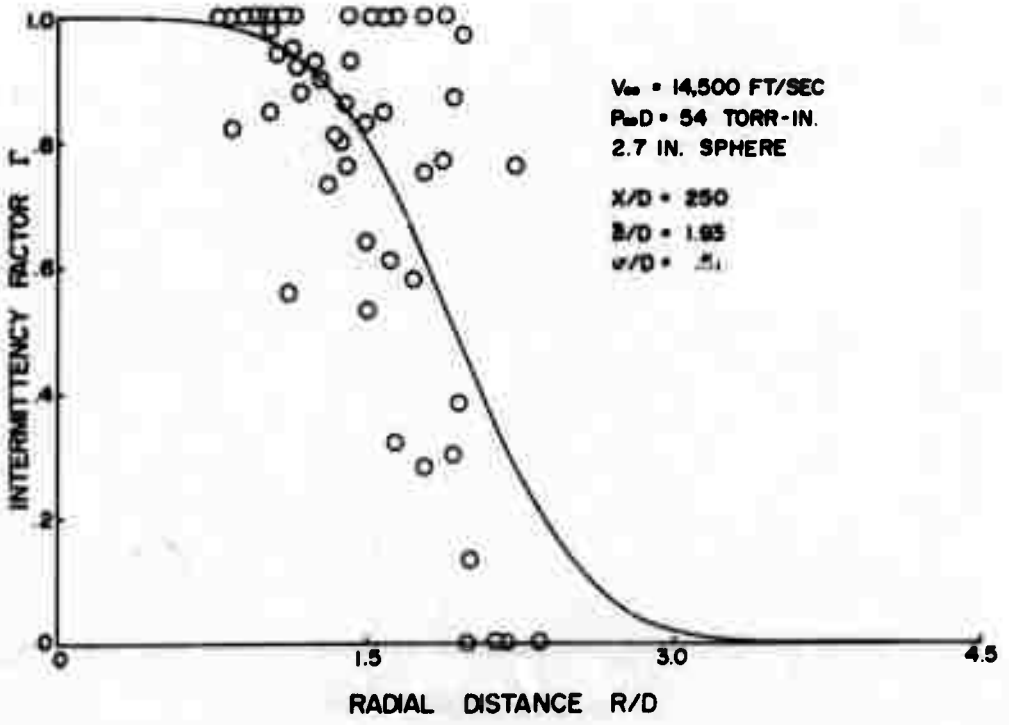

FIGURE B-10

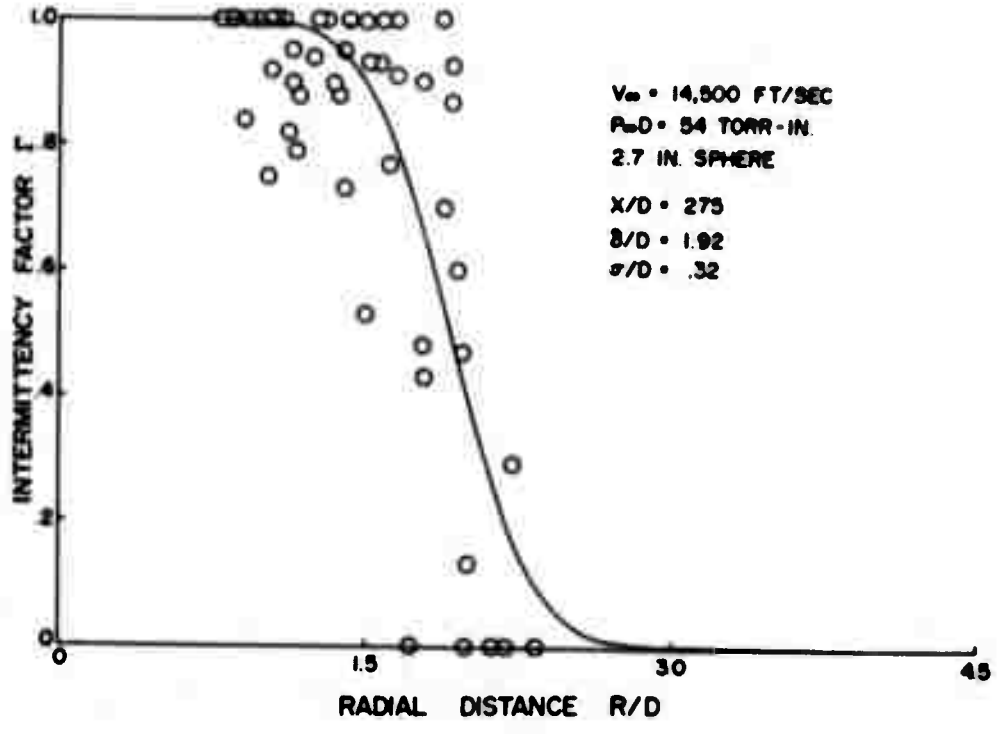

FIGURE B-11

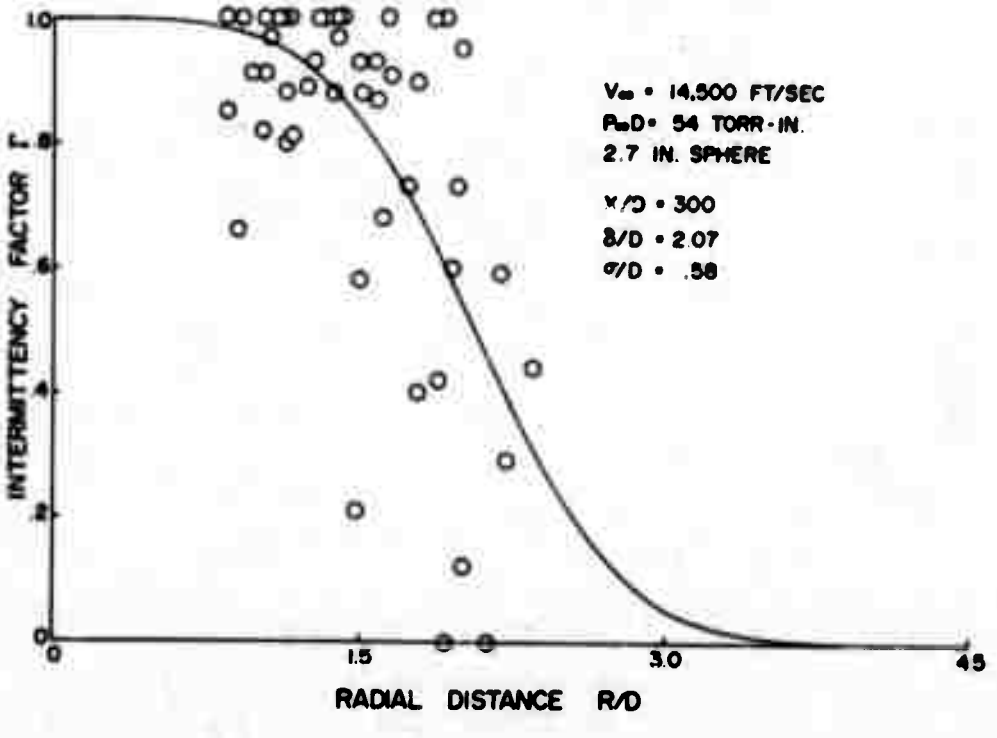

FIGURE B-12

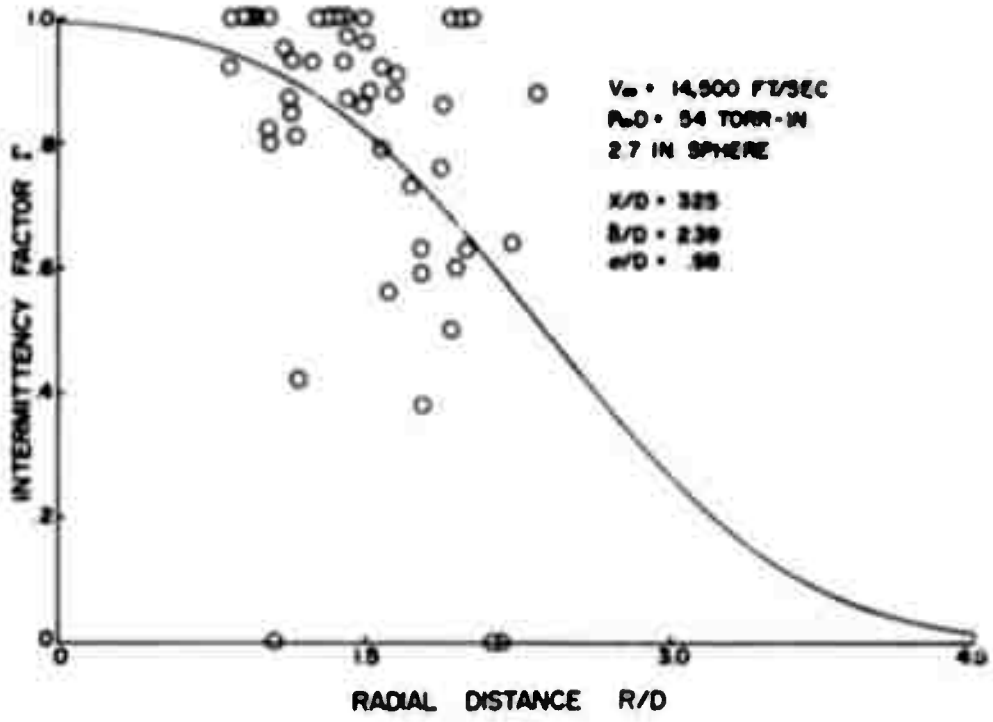

FIGURE B-13

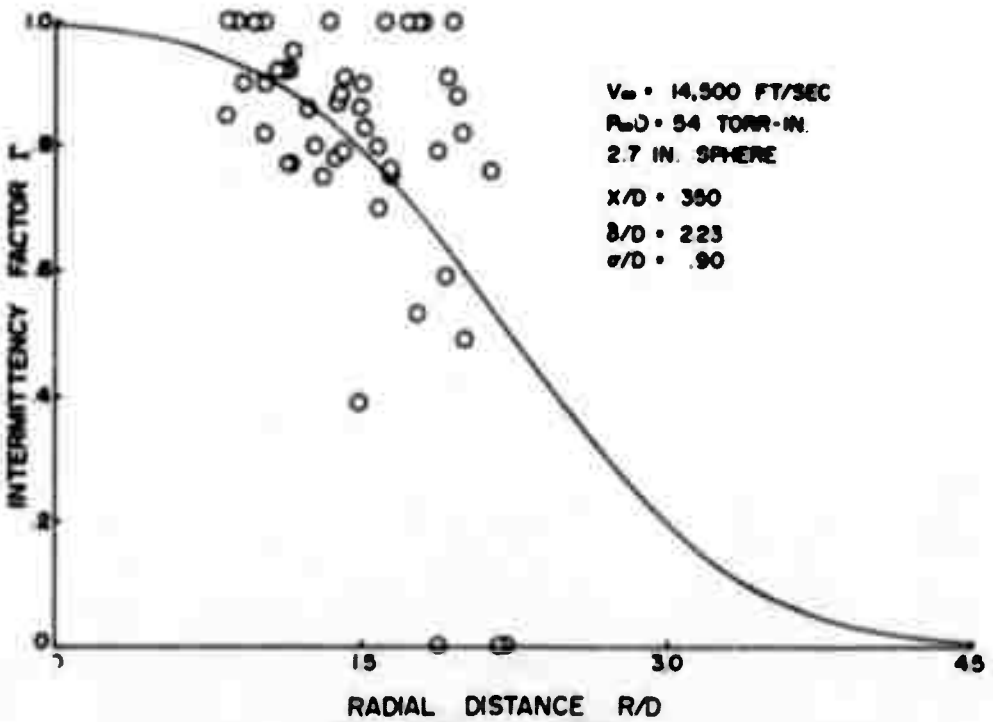

FIGURE B-14

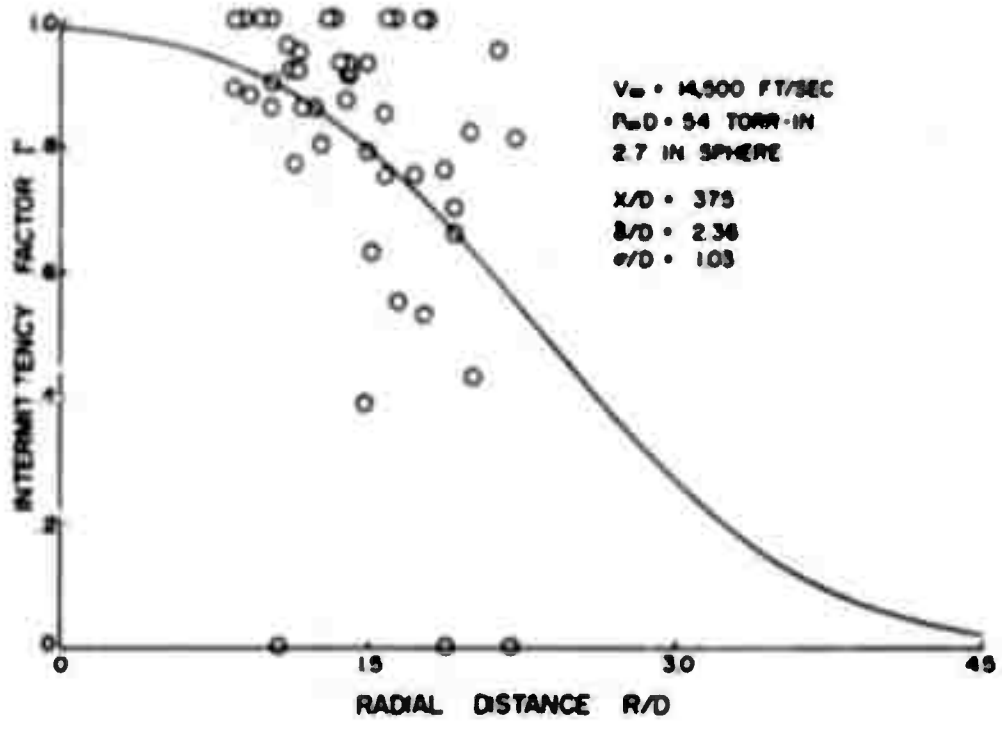

FIGURE B-15

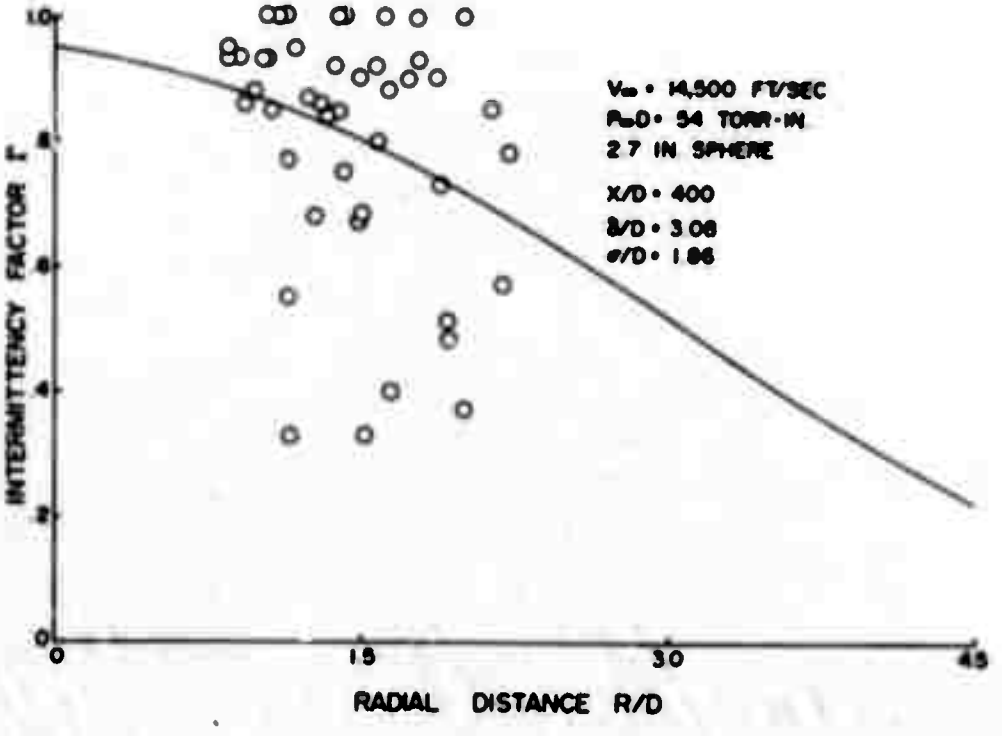

FIGURE B-16

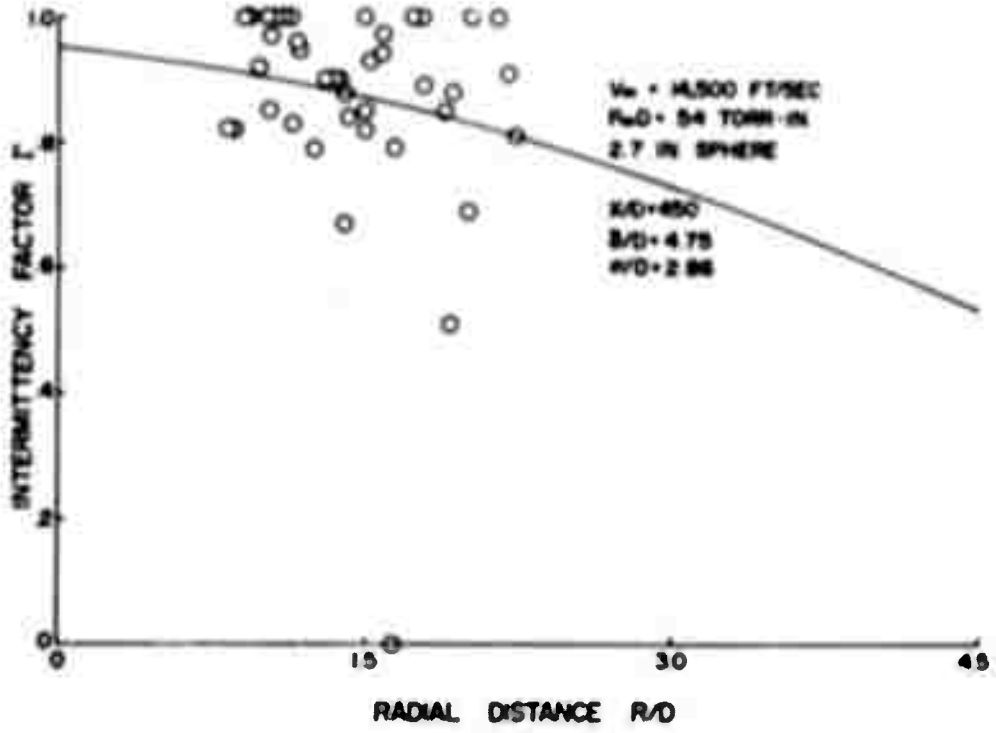

FIGURE B-17

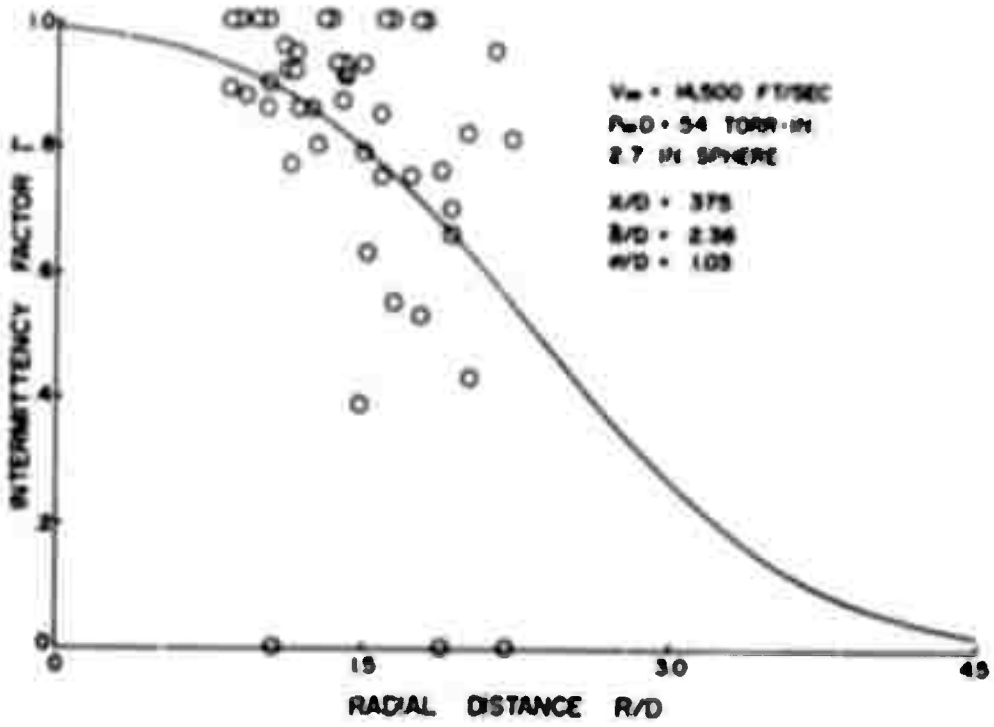

FIGURE B-15

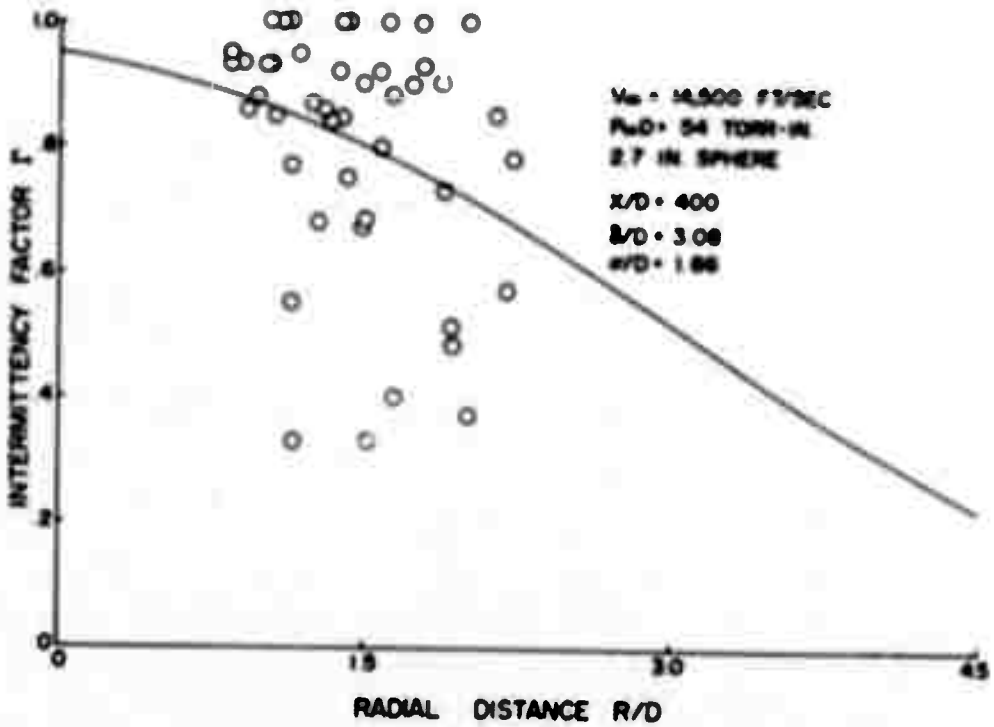

FIGURE B-16

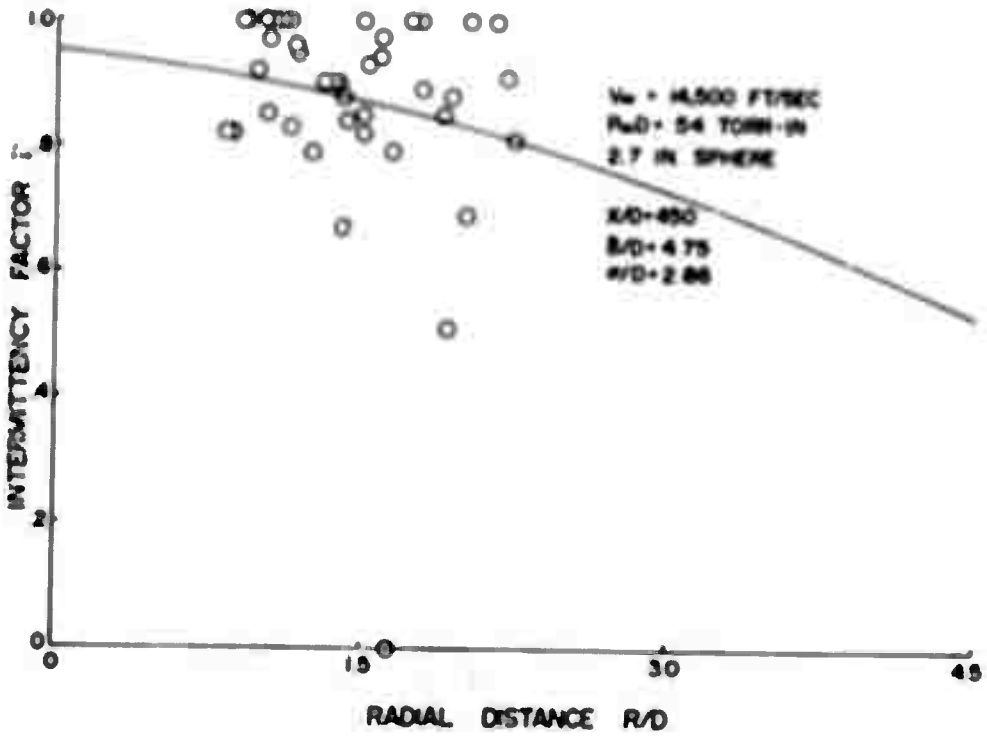
INTERMITTENCY FACTOR γ
RADIAL DISTANCE R/D
0
15
30
45
X/D=4.50
B/D=4.75
W/D=2.86

FIGURE B-17